The minimal cell-cycle control system in *Marchantia* as a framework for understanding plant cell proliferation

Facundo Romani[1,†], Ignacy Bonter[1], Marius Rebmann[1], Go Takahashi[2], Fernando Guzman-Chavez[3], Francesco De Batté[1], Yuki Hirakawa[2], Jim Haseloff[1,†]

[1] Department of Plant Sciences, University of Cambridge, Cambridge, CB2 3EA, UK.

[2] Graduate School of Integrated Sciences for Life, Hiroshima University, Higashi Hiroshima, Hiroshima 739-8526, Japan

[3] Faculty of Chemistry, Food and Biotechnology Department, Universidad Nacional Autónoma de México UNAM, Ciudad Universitaria, Mexico City, 04510, México.

[†] Author for correspondence: fr391@cam.ac.uk, jh295@cam.ac.uk

ABSTRACT

The regulation of cell division is broadly conserved across eukaryotes, governed by cyclins and cyclin-dependent kinases (CDKs) to coordinate progression through the cell cycle. Plants have evolved a complex set of cell-cycle genes with unique features. The high number of cyclin-CDK pairs in flowering plants complicates functional studies due to redundancy and diversification. It is critical to study simple systems in other plant lineages to better understand the functional integration of the cell-cycle control machinery and its evolution across land plants.

Through a comprehensive phylogenetic analysis, we show that non-seed plants possess a simple repertoire of cyclin and CDK proteins, suggesting that the observed complexity in seed plants is a derived trait. The liverwort *Marchantia polymorpha* possesses a streamlined set of core cell cycle genes with minimal redundancy during vegetative development. Using single-cell RNA-seq and fluorescent reporters, we found a precise, phase-specific expression pattern for cell cycle genes. We

demonstrated *in vivo* that only three cyclins are active, one at a given phase, without redundancy. Functional analyses revealed that Mp*CYCD;1* promotes cell cycle re-entry and disrupts differentiation, while overexpression of Mp*CYCA* or Mp*CYCB;1* arrests the cell cycle, consistent with their respective roles at G1, S, and G2/M progression.

Our findings highlight the functional conservation of mechanisms for cell-cycle control across eukaryotes and provide insights into its ancestral state, revealing a minimal set of functional components required for multicellular development. This study advances our understanding of fundamental aspects of cell-cycle regulation and opens new possibilities for engineering plant growth.

Keywords: cell cycle, evolution of development, Marchantia, cyclin-dependent kinases, cyclins.

41 **INTRODUCTION**

42 Eukaryotic organisms have evolved sophisticated mechanisms to control cell
43 proliferation. While cell-cycle control shares common features across eukaryotes, with
44 a conserved set of molecular mechanisms, different lineages such as plants, animals,
45 and fungi adapted it to different multicellular body plans and developmental
46 programmes. Understanding these regulatory networks is a central question for
47 developmental biology and the evolution of development. This knowledge could be
48 instrumental for rational engineering of development and neoorganogenesis in crop
49 plants and promote advances in agricultural biotechnology (Brophy et al., 2018).

50 The eukaryotic mitotic cell cycle progress through G1 (gap 1), S (synthesis), and G2
51 (gap 2) phases to in mitosis (M) (Mironov et al., 1999; Krylov et al., 2003). The
52 transition between phases is governed by a relay of cyclins that activate cyclin-
53 dependent kinases (CDKs) to ensure the proper coordination of replication and
54 chromosome segregation. Group I cyclins are unequivocally associated with cell cycle
55 regulation (Martinez-Alonso and Malumbres, 2020), following an archetypical
56 sequence: D-type cyclins regulate the G1/S transition, A-type cyclins are linked to the
57 S-phase, and B-type cyclins with the G2/M transition (Inze and De Veylder, 2006;
58 Komaki and Sugimoto, 2012). The interaction of cyclins with their CDK partners
59 phosphorylate the retinoblastoma (RB) protein and trigger the transduction of signals
60 necessary for the division of the cells. The regulation of these networks is not only
61 crucial for controlling the rate of cell division but also for maintaining the appropriate
62 balance between proliferation and differentiation, and essential for functional integrity,
63 proper organ formation and integration of environmental responses (Inze and De
64 Veylder, 2006).

65 While the canonical organization of phase specific cyclins/CDKs is well portrayed in
66 the literature and textbooks, most model organisms have different sets of genes that
67 further complicate and specialize this system. For example, animals have E-type
68 cyclins, another G1 specific cyclin that overlaps with D-type, and yeast do not have a
69 true A-type cyclin ortholog. This question is of special importance in plants. The first
70 plant cell cycle components were identified in *Arabidopsis thaliana* as homologs of
71 yeast and animal regulators (Gutierrez, 2009). Plants also exhibit unique cell cycle

features, such as a plant-specific CDKB expressed during G2/M (Gutierrez, 2009). The high complexity of cyclin and CDK regulation, especially in flowering plants, has made it challenging to disentangle their precise functional roles in the progression of the cell cycle in plants (Gutierrez, 2022) and has hindered our ability to understand many fundamental aspects of the cell cycle regulation and evolution.

The Arabidopsis genome displays a large repertoire of cell cycle genes, including 31 Group I cyclins. Among the 10 D-type cyclins, some peak at G1, others at S, and others at G2/M, and only *CYCD3;3* and *CYCD5;1* follow the canonical expression pattern (Menges et al., 2005; Menges et al., 2006). Similarly, expression of the A-type *CYCA3* subfamily peaks at S, while *CYCA1* and *CYCA2* peak at G2/M (Menges et al., 2005). Only B-type cyclins and CDKB genes are consistently expressed at G2/M (Menges et al., 2005). This diversity of expression patterns could be a consequence of gene redundancy and cell cycle specialization. The question of how this system may have worked in early land plant ancestors is yet unresolved.

To understand the plant cell cycle regulation, it is crucial to employ diverse model species. Research in green algae like *Chlamydomonas reinhardtii* has provided critical insights into the fundamental architecture of the cell cycle (Cross and Umen, 2015; Tulin and Cross, 2015; Atkins and Cross, 2018; Breker et al., 2018; Cross, 2020), including conservation of the regulation of the anaphase-promoting complex by the plant specific CYCB/CDKB complex (Pecani et al., 2022). However, *Chlamydomonas* exhibit an uncommon multiple-fission cell cycle, that consists of a long G1 phase followed by successive rounds of S phases and M (Cross and Umen, 2015), making it hard to compare with other plant species. Non-vascular plants offer a promising opportunity to study the cell cycle in early divergent plants, with different cellular body plans. The moss *Physcomitrium patens* has revealed both conserved and unique aspects of plant cell cycle regulation (Schween et al., 2008; Ishikawa et al., 2011; Peramuna et al., 2023). However, the large repertoire of cyclins and CDKs in *Physcomitrium* creates challenges for understanding due to functional redundancy.

The model liverwort *Marchantia polymorpha*, features a reduced set of cell-cycle regulators (Bowman et al., 2017). Its simplicity positions Marchantia as a key organism to study the evolution of developmental and systems biology (Bowman et

103 al., 2022; Romani et al., 2024) and could be instrumental to understand the evolution
104 of the cell-cycle control system across land plants without the confounding effects of
105 gene redundancy and sub-functionalization. However, functional studies in this
106 species are lacking.

107 In this work, we made a comprehensive phylogenetic analysis of cell cycle genes
108 across plants and other eukaryotes and observed that Marchantia retains a minimal
109 set of regulators. Expression profiles and functional analyses allowed us to elucidate
110 the organization of the core cell cycle regulation genes that operate in Marchantia and
111 compare this system with its counterparts in other eukaryotes. Functional analyses of
112 cyclin genes in the Marchantia vegetative gametophyte revealed that Mp*CYCD;1* is a
113 rate-limiting factor for cell proliferation, promoting dedifferentiation, while Mp*CYCB;1*
114 and Mp*CYCA* causes cell cycle arrest. On the other hand, MpCYCB;2 is a gene in the
115 process pseudogenization and MpCYCD;1 is not a canonical D-type cyclin, without
116 any significant impact in plant growth. Overall, these results provide a model of the
117 streamlined cell-cycle control system in Marchantia and will be useful to navigate study
118 of the cell cycle and future approaches to engineering plant growth and development.

119

120 **RESULTS**

121 **Phylogenetic analysis of core cell cycle genes**

122 To investigate the core regulation of cell cycle regulation in land plants, we conducted
123 a phylogenetic analysis of cell cycle genes in a broad range of 27 eukaryotic species,
124 including yeast, animals, brown and red algae, charophytes, bryophytes, lycophytes,
125 ferns, and flowering plants (Figure 1). We focused on gene families that have been
126 described as fundamental components of the cell-cycle control machinery, including:
127 Group I cyclins, CDKs, CYCLIN-DEPENDENT KINASES REGULATORY SUBUNIT
128 (CKS), RETINOBLASTOMA-RELATED (RBR) proteins, and the associated
129 transcription factors (TFs) from the E2F, DP, DEL, and 3R-MYB gene families.

130 A-, B-, and D-type cyclins are well conserved across eukaryotes, except fungi, which
131 only display two classes of cyclins (Ma et al., 2013) corresponding to the B- and D-
132 type (Figure 1a,c). E-type cyclins are specific to animals, with potential presence in

133 other green algal lineages but absent in land plants (Figure 1a-b). SOLO DANCERS
134 (SDS) cyclins are a group of plant-specific cyclins associated with meiosis (Azumi et
135 al., 2002) that likely originated in charophytic algae but those genes were
136 subsequently lost in some non-seed plants (Figure 1c). Interestingly, there is a gene
137 duplication of the D-type cyclins that appear to have given rise to a new clade of
138 bryophyte-specific cyclins that we named CYCD' (Figure 1a,c).

139 CDKAs and CDKBs are the main partners that interact with cyclins to help govern cell-
140 cycle progression in plants. CDKA, homologous to yeast CDC28, is conserved across
141 eukaryotes with the hallmark PSTAIRE motif (Figure 1b-c, Suppl. Figure 2). The G2/M
142 specific CDKB is ubiquitously present in all green plants (Figure 1b-c). In non-flowering
143 plants, they are associated with the PSTALRE motif (Figure 1b) that is well conserved
144 across the family, as opposed to the P(P/S)T(A/T)LRE in flowering plants (Joubes et
145 al., 2000). The only case in which this motif is found in CDKBs outside the green algae
146 are the brown algae, *Ectocarpus siliculosus*, which contain two divergent CDKB-like
147 CDKs with the PSTALRE motif (Figure 1b).

148 Other CDKs can act as activators within the cell cycle phosphorylation cascade
149 (Joubes et al., 2000). CDKC (homologous to yeast CTK), CDKD (KIN28), CDKE
150 (CAK1/SSN3), and CDKG are conserved across eukaryotes, with some lineage-
151 specific losses (Figure 1b-c). Notably, the CDKC subfamily has expanded in plants,
152 forming a distinct streptophyte-specific CDK-like clade, whose function is largely
153 unknown. (Joubes et al., 2000). Among the remaining clades, CDKF is found in all
154 streptophytes, and the PHO85 clade, which belong to the CDKA/CDC28 super-family,
155 is conserved in yeast and animals but not found in most other eukaryotes (Liu and
156 Kipreos, 2000). Divergent CDKAB members form a paraphyletic group in scattered
157 species, lacking conserved motifs. CKS genes are broadly conserved, except in the
158 charophyte algae *Mesostigma viridae* (Figure 1c).

159 Downstream of CDK signalling, the RBR pathway is essential for cell cycle progression
160 and is also highly conserved, with a single RBR homologue in most species. There
161 are three clades of RBR-related TFs that form part of the DREAM complex during the
162 G1/S transition (E2F, DP, and DEL). The three clades share a common evolutionary
163 origin (Rauber et al., 2016). E2F and DP TFs form highly conserved heterodimers to

regulate the onset of DNA replication. Both protein families are present in animals and plants, suggesting an early origin of the interaction (Figure 1c). In contrast, DEL proteins, which are present in both brown algae and plants, have been lost in several plant lineages.

The 3R-MYB TFs (or c-Myb in animals), which regulate the G2/M transition (Ito et al., 2001), show a common origin before the divergence of plants and animals (Kobayashi et al., 2015; Feng et al., 2017), with some lineages losing one of the MYB domains. All plant species contain at least one 3R-MYB gene, except for the algae species *Chlamydomonas* and *Penium margaritaceum* (Figure 1c).

In charophytes, including the algal sister lineage of land plants (Feng et al., 2024), and bryophytes, most cell-cycle genes exist as single copies, suggesting that the common ancestor of land plants possessed a minimal set of these core components. This set has expanded considerably in some lineages, particularly in flowering plants, consistent with the pattern of whole-genome duplications. Remarkably, the liverwort *Marchantia polymorpha* retains a simplified set of cell cycle regulators, with highly reduced redundancy compared to vascular plants. It has single copies of most cell cycle regulators, except for CYCD (Mp*CYCD;1* and Mp*CYCD;2*) CYCB (Mp*CYCB;1* and Mp*CYCB;2*), and CDKC (MpCDKC;1 and MpCDKC;2), and a considerable repertoire of TFs, including 3 DP (Mp*DP1*, Mp*DP2*, and Mp*DP3*), 2 DEL (Mp*DEL1* and Mp*DEL2*), and 9 3R-MYBs (Mp*3R-MYB1* to Mp*3R-MYB9*).

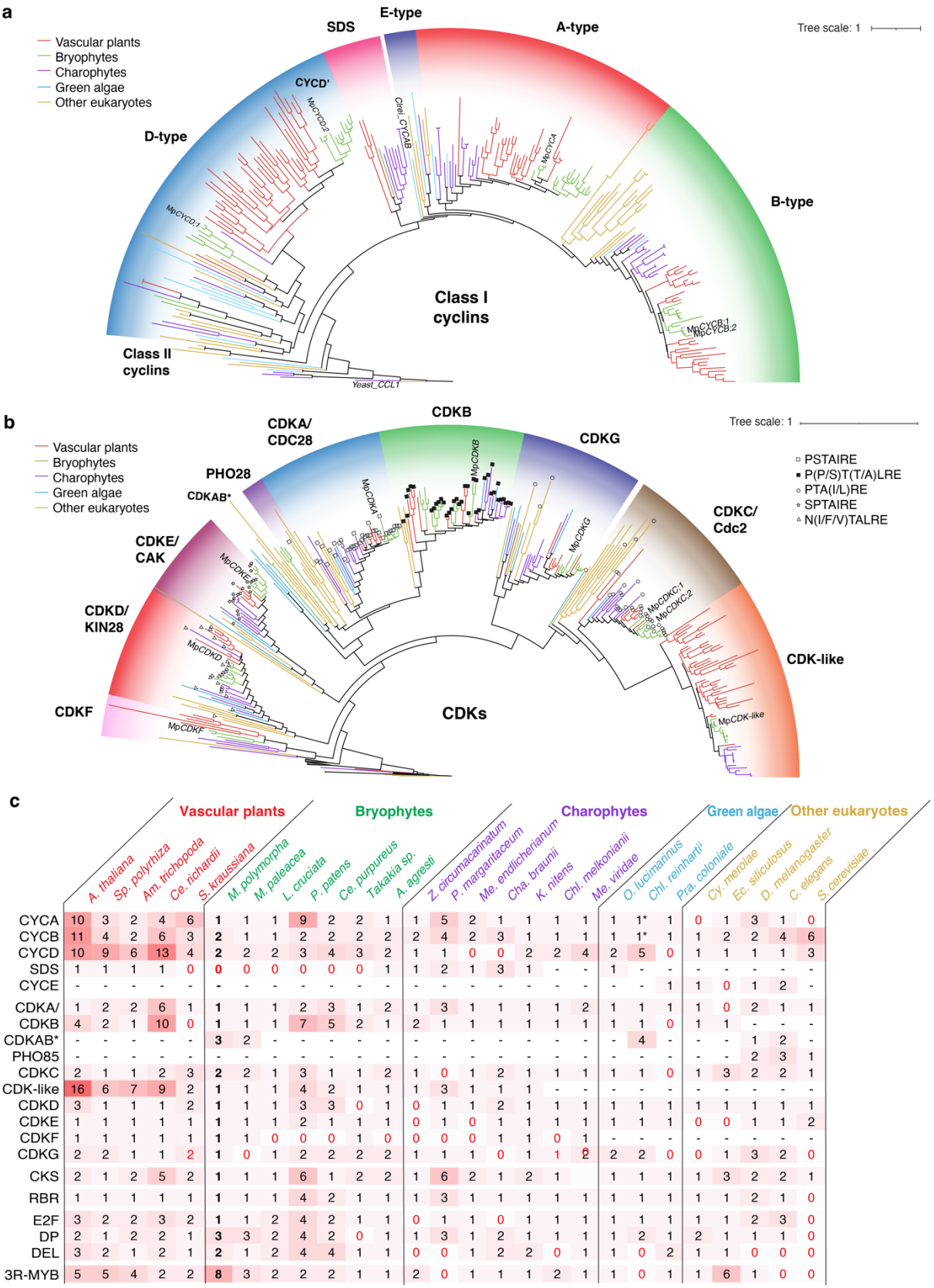

185

186 ***Figure 1. Phylogenetic analysis of core cell cycle genes across eukaryotes.*** *a-b)*

187 *Maximum likelihood Phylogenetic analysis of cyclins across representative plant and*

188 *eukaryotic species. (a) and CDKs (b). In each diagram, subfamilies are indicated with*
189 *different shaded background colours. Branches are coloured according to species in*
190 *each clade as shown in the figure legends. Conserved signature motifs across CDKs*
191 *are indicated in each node as shown in the figure key on the right. Full phylogenies*
192 *and details are available at Suppl. File 1. c) Summary of the number of cell cycle genes*
193 *across eukaryotic species. Background colour indicates the total number of genes in*
194 *darker red. Hyphens indicate absence, while red zeros indicate potential losses. **
195 *Chlamydomonas reinhardtii has an extra divergent CYCAB1 (Cre08.g370401).*

196

197 **Expression profile of cell-cycle genes in Marchantia**

198 To investigate the dynamic expression of key cell-cycle regulators in Marchantia, we
199 re-analysed RNA-seq time-series data from two natural biological processes that
200 feature a semi-synchronized re-entry to the cell cycle: meristem regeneration (Ishida
201 et al., 2022) and sporeling germination (Bowman et al., 2017). During regeneration,
202 cells begin proliferating approximately 16 hours after meristem excision (Nishihama et
203 al., 2015). Similarly, dormant spores start dividing between 29 and 48 hours after
204 exposure to light (Attrill et al., 2024).

205 During sporeling germination Mp*CYCD;1* transcripts accumulated after 24 hours of
206 light exposure, before the first cell division, followed by peaks in Mp*CYCB;1*, Mp*CYCA*,
207 Mp*CDKB*, Mp*CKS* at 48 hours (Figure 2a). We also employed *HISTONE H3.1*
208 (Mp*H3.1)* transcript accumulation as a reference marker for DNA replication, which
209 also peaked 48 hours after light exposure. A similar pattern was observed during
210 regeneration (Figure 2b), consistent with previous reports (Nishihama et al., 2015).
211 These findings are consistent with a role for Mp*CYCD;1* in G1, driving cell cycle re-
212 entry, and highlight other genes that are induced during cell cycle progression. On the
213 other hand, Mp*CDKA*, other CDKs, Mp*RBR,* and Mp*CYCD;2* remained constitutively
214 expressed (Figure 2, Suppl. Figure 1, Suppl. Figure 2). Mp*E2F* and Mp*DP1*
215 transcription factors showed moderate but detectable upregulation (Figure 1a-b).

216 Some predicted cell-cycle genes showed low or no detectable expression during both
217 regeneration and sporeling germination, including: Mp*CYCB;2, MpCDKAB;1-3,* and
218 Mp*DP2 MpDP3* (Figure 1, Suppl. Figure 1). Mp*3R-MYB1* remained the most

219 abundantly expressed *3R-MYB* ortholog in the vegetative gametophyte. By contrast,
220 Mp*3R-MYB3* to Mp*3R-MYB9* were specifically expressed during early sporophyte
221 development, and Mp*3R-MYB7* and Mp*3R-MYB8* were detected at the spore stage
222 too (Suppl. Figure 1). These 3R-MYB homologues belong to a different clade
223 compared to 3R-MYB1 expressed in the gametophyte (Suppl. Figure 1). Something
224 analogous was observed with Mp*DEL2*, which is expressed in the antheridium (Suppl.
225 Figure 1). These data suggest that in the vegetative gametophyte, a simplified cell
226 cycle regulation network is active, with only one copy of each TF. While in the
227 sporophyte and during gametogenesis, some specialization could be expected.

228 To further investigate the spatial distribution of cell divisions and growth, we focused
229 on the early stages of Marchantia gemma development. The meristem undergoes a
230 transition from an immature state to the fully mature state around 5-days post-
231 germination (Romani et al., 2024). We performed 5-ethynyl-2'-deoxyuridine (EdU)
232 staining to label actively dividing cells. As expected, EdU-positive cells were
233 concentrated around the division and differentiation zones (DDCZ) and the stem-cell
234 zone (SCZ), including the apical cell (Figure 3a-b). This is the main focal point for
235 growth in Marchantia, with a very simple architecture. Cells near the apical notch
236 proliferate and differentiate, forming specialized cells and air pore structures.
237 Epidermal cells exit the cell cycle and elongate as they become distal to the apical
238 notch (Figure 3a-b).

239 To elucidate the expression of cell cycle regulators during gemmaling development,
240 we generated transcriptional reporters using Golden-Gate compatible constructs
241 (Sauret-Gueto et al., 2020; Romani et al., 2024). Transcriptional reporters showed that
242 most key components were actively expressed in the EdU-positive zone (Suppl. Figure
243 3), corresponding to the DDCZ of the vegetative meristem. Consistent with the
244 transcriptomic analysis, the promoter of Mp*CYCB;2* showed no detectable expression,
245 suggesting it could be a pseudogene. *pro*Mp*CYCD;2* exhibited a more irregular pattern
246 compared to *pro*Mp*CYCD;1*, which was consistently expressed in dividing cells. TFs
247 linked to cell cycle regulation, including Mp*3R-MYB1*, and Mp*E2F,* followed expected
248 expression patterns based on prior transcriptomic analyses in the gametophyte
249 (Suppl. Figure 3). Expression of DP TFs reporters was not detectable at this stage
250 (Romani et al., 2024). This is inconsistent with Mp*DP1* transcriptomics, likely due to

251 the promoter being insufficient to capture all regulatory elements important for this
252 gene.

253

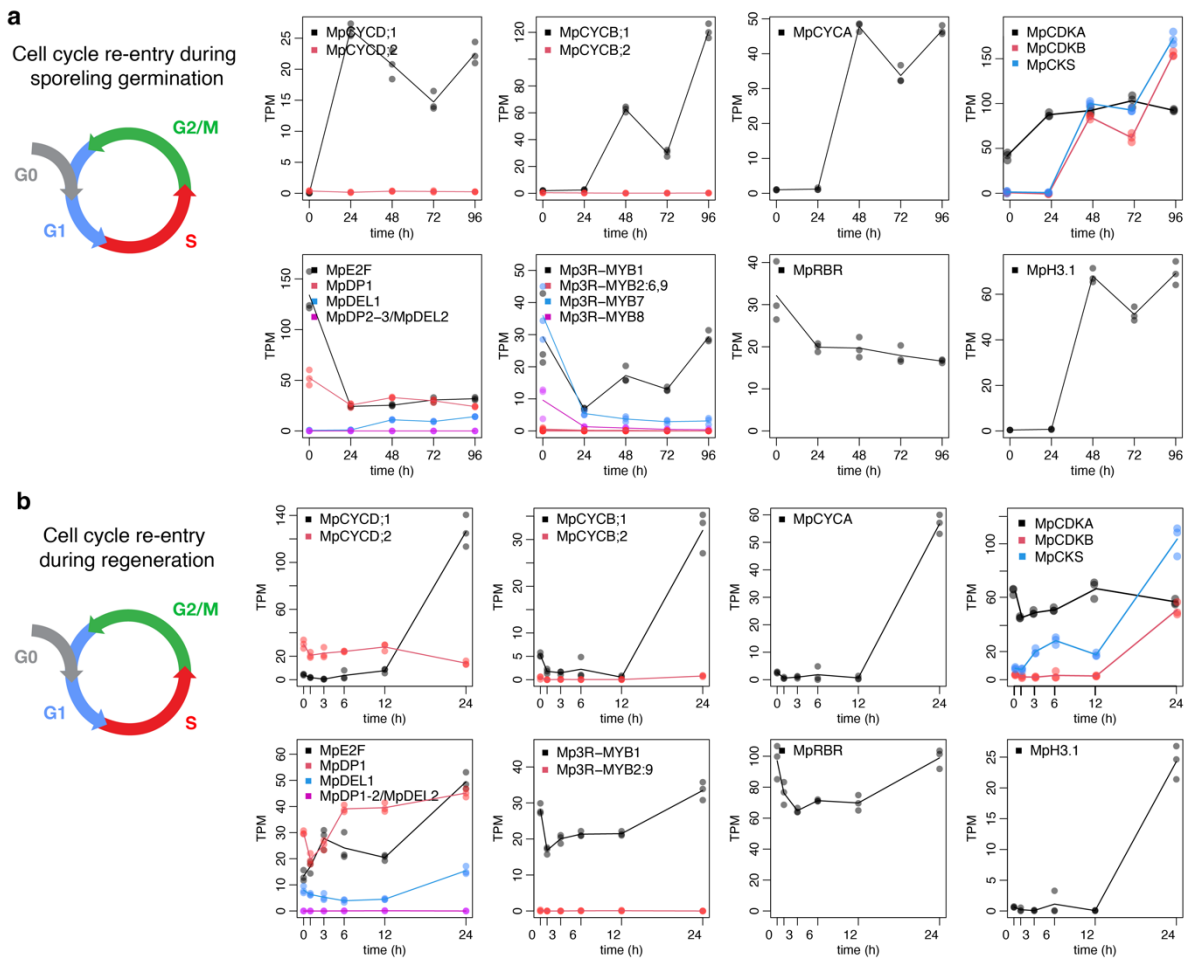

254

255 ***Figure 2. Expression of core cell cycle genes in Marchantia during re-entry.*** a-b)
256 *RNA-seq analysis of representative cell cycle genes during the time course of*
257 *sporeling germination (a) and regeneration (b). Genes are grouped per families and*
258 *distinguished by colour (see legend). Individual points represent biological replicates*
259 *and lines averages.*

260

261 **Phase specificity of cell-cycle genes**

262 To gain a more refined understanding of the dynamic expression of cyclins during all
263 phases of the cell-cycle, we leveraged single-cell RNA-seq data obtained from growing
264 gemmalings. Previous work identified clusters of cells proliferating around the apical

265 notch, including cell cycle related genes (Wang et al., 2023). Sub-clustering of this
266 group revealed three clearly distinct expression profiles (Figure 3c). Using well-known
267 markers, we labelled sub-clusters corresponding to G0/G1, S, and G2/M phases and
268 identified a comprehensive set of additional phase specific markers (Suppl. Table 1).
269 The G0/G1 sub-cluster was characterized by the expression of Mp*CYCD;1*, Mp*CDKA*,
270 and Mp*MCM3*, homologues of *Arabidopsis* G1-phase markers (Zhang et al., 2021)
271 and other genes associated G1 and initiation of replication (Figure 3c). The S-phase
272 cluster was defined by replication-related genes, including Mp*CYCA*, several histones,
273 and DNA damage repair genes such as Mp*RAD51*. The G2/M sub-cluster showed
274 elevated expression of mitotic markers, including the single CDH1 unit of the
275 Anaphase Promoting Complex/Cyclosome (APC/C) present in Marchantia
276 (Mp*CCS52A1),* both *CDC;20* cofactors (Mp*CDC20;1* and Mp*CDC20;2*) (Figure 2e-f),
277 and key core cell-cycle genes: Mp*CDKB,* Mp*CKS,* and Mp*3R-MYB1*. Among the other
278 CDKs, Mp*CDKD* showed differential expression in the G2/M cluster and Mp*CDKG* and
279 Mp*CDK-like* in G0/G1, similar to their homologues in *Arabidopsis* (Menges et al.,
280 2005). Transcript levels of other key components of the cell cycle such as RBR and
281 CKIs did not show preferred accumulation in specific phases of the cell-cycle.

282

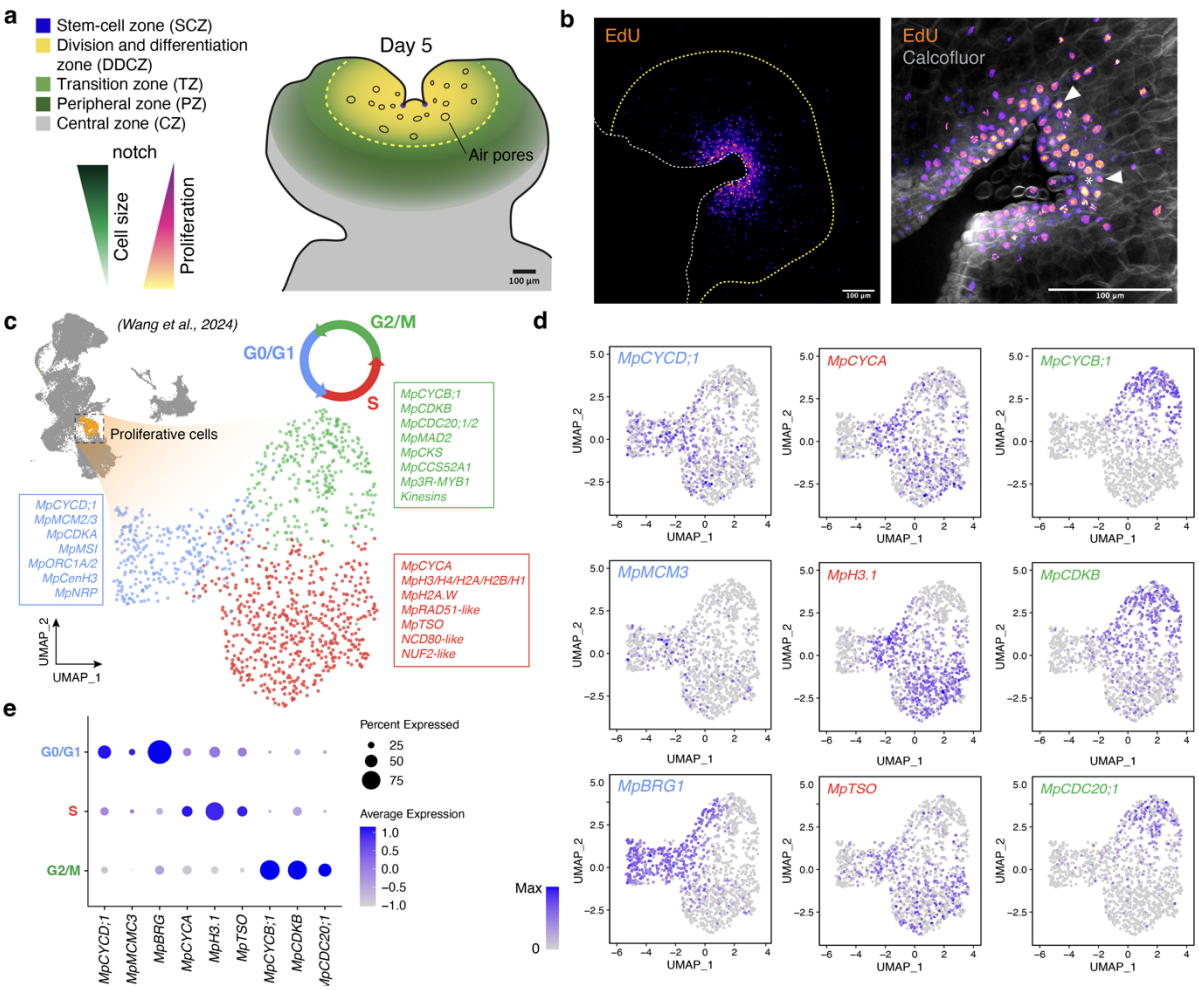

Figure 3. **Gene expression fluctuations during cell proliferation *in Marchantia.*** *a) Diagram of cellular domains associated with cell proliferation in the Marchantia gemmaling b)* 5-ethynyl- 2'-deoxyuridine (*EdU) staining of the Marchantia meristem in 5-days old gemmalings. The white dashed line delimitates the outline of the plant. The yellow dashed line represents the boundary of the mature epidermis.* Scale bar is shown in each image. *c-e)* UMAP of scRNA-seq of Marchantia proliferative cells subcluster. The UMAP including all cells is shown in the top left corner for reference. Proliferative cells are highlighted in orange. e) UMAP of the proliferative cells and classification into 3 sub-clustering (G0/G1, light blue; S, red; and G2/M, green). Feature plots (d) and dot plot (e) of representative genes are shown in coloured square legends. Abbreviations: *MCM (MINICHROMOSOME MAINTENANCE), CDC (CELL DIVISION CYCLE PROTEIN HOMOLOGUE), MSI (MUSASHI), ORC (ORIGIN RECONGNITION PROTEIN), CCS52A (CELL CYCLE SWITCH PROTEIN 52 A), NDC (NUCLEAR DIVISION CYCLE), NUF (KINETOCHORE PROTEIN NUF),*

298 *BRG (BLEOMYCIN RESISTANT GENE), NRP (NAP-RELATED PROTEIN). TPM,*
299 *transcripts per million; asinh, inverse hyperbolic sine.*

300

301 Cyclins are not only subjected to tight transcriptional control during cell division, but
302 also protein degradation. We made translational reporters for MpCYCD;1/2,
303 MpCYCB;1, MpCYCA and MpCDKA to better capture the protein expression dynamics
304 during cell division. These protein fusions correspond to the CDS and a C-terminal
305 mVenus (mV) fluorescent protein. Compared to promoter fusions for the
306 corresponding genes, the signals are more restricted to dividing cells. MpCYCD;1 is
307 highly expressed in dividing cells as expected, and rhizoid precursors and air pores
308 (Figure 4a, Suppl. Figure 4a). On the other hand, MpCYCD;2 translational reporter
309 was undetectable in vegetative tissues. MpCYCB;1 has the typical “salt and pepper”
310 (Figure 4a) as described in its homologues in flowering plants (Schnittger et al.,
311 2002a). A similar pattern was observed for MpCYCA (Figure 4a). MpCDKA
312 translational reporter is broadly expressed across the mature thallus and not restricted
313 to dividing cells (Suppl. Figure 5a). Finally, MpCDKB is more restricted to dividing cells
314 (Suppl. Figure 5b).

315 For time-lapse imaging, we took advantage of cell cycle re-entry occurring during
316 regeneration, which allows a clear visualization of the cellular features associated with
317 its expression dynamics during cell division using the translational reporters. Live
318 imaging showed that MpCYCD;1 protein accumulated in the nuclei of cells before cell
319 division and was rapidly degraded before the start of the prophase (Figure 4a, Suppl.
320 Video 1). Similarly, MpCYCA also accumulated in the nuclei until the prophase and
321 was rapidly released to the cytosol and degraded (Figure 4b, Suppl. Video 2). Finally,
322 MpCYCB;1 was transiently expressed in the cytosol and accumulated during
323 metaphase/anaphase, and signal was rapidly lost before cell plate formation (Figure
324 4c, Suppl. Video 3). Intriguingly, MpCYCB;1 was re-localized to the nuclei before loss
325 of signal, likely due to degradation. The translocation of B-type cyclins during the
326 metaphase-anaphase has been well described in animal cells (Clute and Pines, 1999)
327 with the export of CYCB from the nucleus to the cytosol (Toyoshima et al., 1998). To
328 our knowledge, this is the first report of this type of translocation in plant cells.

329 We also looked at translational reporters for MpCDKA and MpCDKB. Both were
330 localized in the cytosol and nucleus and fluorescence was visible throughout the cell
331 cycle. While MpCDKA strongly accumulated in the interphase (Suppl. Figure 6a,
332 Suppl. Video 4), MpCDKB was found more prominent later in the prophase and during
333 mitosis (Suppl. Figure 6b, Suppl. Video 5). Overall, these results align with the
334 respective roles of the main cyclins and CDKS in Marchantia in the progression of the
335 cell cycle. This also highlights the importance of protein degradation and nuclear
336 export/import in controlling cyclin-dependent activity.

337

338

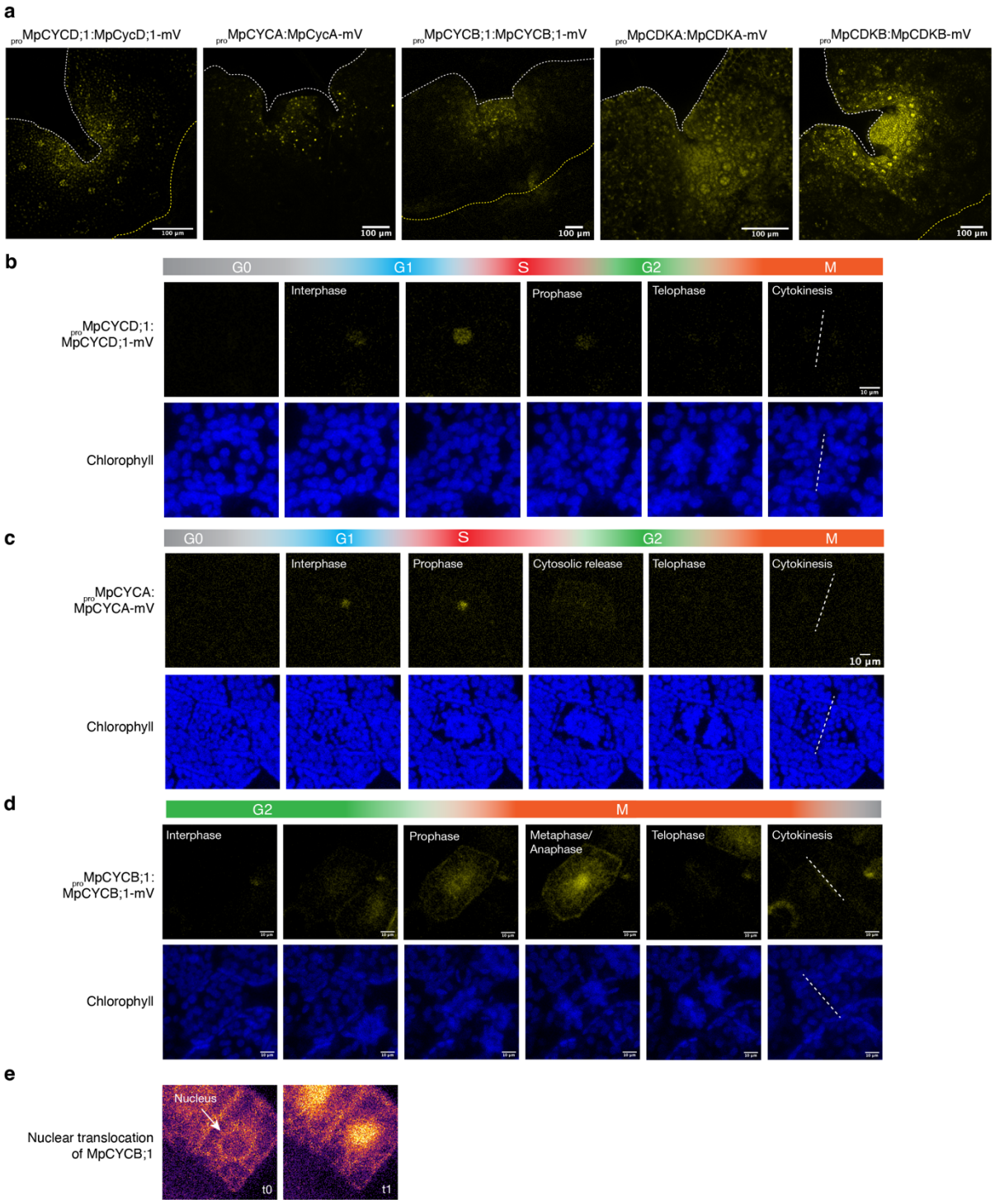

339

340 ***Figure 4. In vivo expression of cyclins and CDKs in Marchantia.*** Expression of
341 cyclin and CDKs translational reporters (yellow) in 5-days old gemmalings. b-d) Time-
342 lapse of MpCYCD;1 (b) MpCYCA (c), and MpCYCB;1 (d) translational reporters of an
343 individual cell dividing during regeneration (yellow). Chlorophyll (blue) is shown to
344 visualize the cell division phases using chloroplast movement. d) The translocation of

345 MpCYCB;1 (inferno LUT) from the cytosol to the nuclei at two different frames. The
346 full videos of the time-lapses are available at Suppl. Video 1-3. *The white dashed lines*
347 *delimit the outlines of the plants. The yellow dashed lines mark the boundary of the*
348 *mature.* Scale bars of the indicated sizes are shown in each image.

349

350 **Functional analysis of cyclins in Marchantia**

351 We generated fluorescent protein fusions (CDS-mVenus) for overexpression of cyclins
352 and CDKA. MpCYCD;1 is localized in the nucleus as most D-type cyclins in
353 *Arabidopsis,* while MpCYCD;2 showed a broader distribution in the cytosol (Figure
354 5a). As shown before, CDKA is cytosolic (Figure 5a) as its orthologue in *Arabidopsis*
355 (Boruc et al., 2010). Constitutive overexpression of Mp*CYCD;1* resulted in smaller
356 plants with reduced cell size and severe developmental defects (Figure 5b). In
357 contrast, overexpression of Mp*CYCD;2* or Mp*CDKA* had no noticeable effect on plant
358 growth (Figure 5c).

359 Mp*CYCB;1* and Mp*CYCB;2* share high sequence similarity (90.1 %), but Mp*CYCB;2*
360 lacks the conserved intron structure, and its endogenous expression is undetectable
361 (Figure 2, Suppl. Figure 1, Figure 5b). Both B-type cyclins localize in the cytosol and
362 nucleus (Figure 5a), consistent with its homologues in *Arabidopsis* (Boruc et al., 2010).
363 Overexpression of either Mp*CYCB;1* or Mp*CYCB;2* impaired growth, resulting in
364 smaller plants (Figure 5d). This indicates that despite signs of pseudogenization,
365 Mp*CYCB;2* encodes for a functional protein. Imaging of plants overexpressing
366 MpCYCB;1 revealed that cells with higher mVenus signal were arrested in mitosis at
367 a metaphase-like stage (Figure 5h, Suppl. Video 6), unlike the transient expression
368 observed native promoter control (Suppl. Video 7).

369 We also generated lines with inducible expression of Mp*CYCD;1*, Mp*CYCD;2*,
370 Mp*CYCB;1* Mp*CYCA* using an β-estradiol XVE system under the control of $_{pro}$MpE2F
371 (Siligato et al., 2016; Ishida et al., 2022). Inducible overexpression of MpCYCD;1
372 further confirmed its role in controlling cell division, producing ectopic cell division and
373 hyperplasia (Figure 5e,f), evidenced by significantly smaller cells under induction
374 (Figure 5g) lacking proper differentiation. Under this setting, inducible overexpression
375 of Mp*CYCD;2* did not cause any conspicuous developmental defect. On the other

hand, inducible overexpression of Mp*CYCB;1* caused cell death. Inducible expression of Mp*CYCA* also caused a similar phenotype, suggesting that its accumulation is also arresting cells at mitosis (Figure 5g). This supports the key role of Mp*CYCB;1* and Mp*CYCA* in cell cycle control, while their degradation is required for the proper progression of cytokinesis.

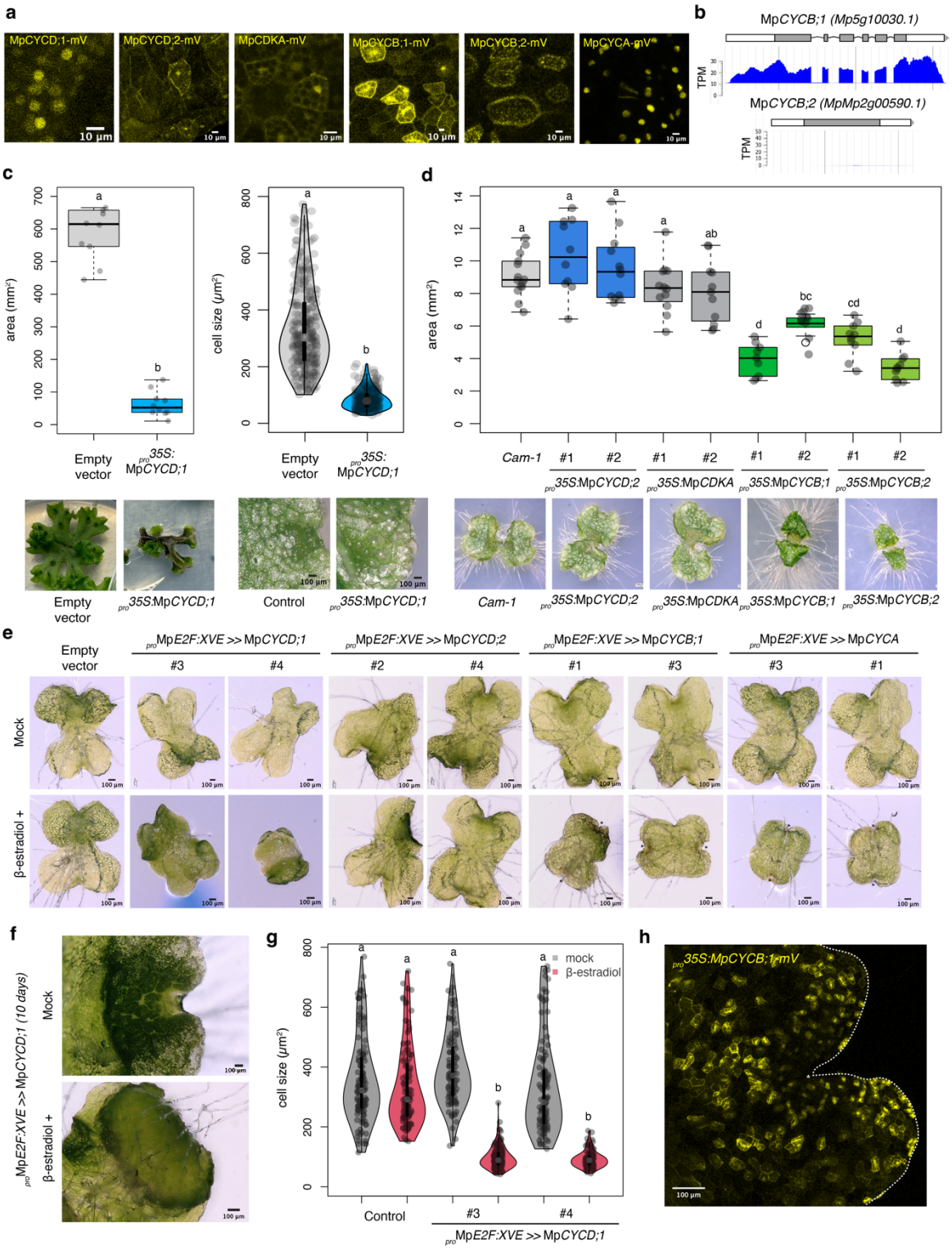

382 ***Figure 5. Functional characterization of cyclins and CDKA.*** *a) Subcellular*
383 *localization of selected cyclins and CDKA protein fusions with mVenus. b) Overview*
384 *of the genomic locus of* Mp*CYCB;1 and* Mp*CYCB;2, including a diagram of intron*
385 *structure and average RNA-seq coverage in mixed tissues. c) Boxplot of plant area*
386 *(left) and cell size (right) of* $_{pro}$*35S:*Mp*CYCD;1-mVenus primary transformant plants.*
387 *Representative pictures of the plants are shown. d) Boxplot of plant area of*
388 $_{pro}$*35S:*Mp*CYCD;2-mVenus,* $_{pro}$*35S:*Mp*CDKA-mVenus,* $_{pro}$*35S:*Mp*CYCB;1-mVenus,*
389 *and* $_{pro}$*35S:*Mp*CYCB;2-mVenus constitutive overexpression at 7 days. Representative*
390 *pictures of the plants are shown at the bottom. e) Representative pictures of*
391 *gemmalings of transgenic plants with inducible overexpression of cyclins grown for 3*
392 *days or 10 days (f) in 0.5x Gamborg B5 supplemented with 5 µM β-estradiol (EST+)*
393 *or DMSO (mock). Transgenic constructs are indicated in the images. g) Violin plots of*
394 *cell size of inducible* Mp*CYCD;1 (*$_{pro}$*MpE2F:XVE>>MpCYCD;1). in 3-days old plants.*
395 *f) Confocal microscopy of* $_{pro}$*35S:*Mp*CYCB;1-mVenus (yellow) overexpression. The*
396 *white dashed line delimitate the outline of the plant. The yellow dashed line represents*
397 *the boundary of the mature epidermis. Control indicates a transgenic line transformed*
398 *with an empty vector.* Scale bar lengths are indicated in the pictures. Symbols above
399 the bars indicate grouping by P-value<0.001 in a Tukey's Honest Significant
400 Difference method.

401

402 Finally, to examine whether Mp*CYCD;2* play any physiological role for Marchantia
403 vegetative development, we generated CRISPR-Cas9 knock-out lines. We obtain
404 independent lines using two different gRNAs, generating a 20 bp (Mp*cycd;2-1*^{ge}) or 1
405 bp (Mp*cycd;2-2*^{ge}) deletions (Figure 6a, Supplemental Figure 7) that causes early stop
406 codons. We did not find any significant defect in plant growth (Figure 6b) compared to
407 wild-type plants. Considering overexpression results, this suggest that Mp*CYCD;2*
408 does not affect cell proliferation and could be a pseudogene.

409

410 **Cell Proliferation Interferes with Differentiation**

411 Morphological defects observed after Mp*CYCD;1* overexpression showed that cell
412 differentiation was disrupted when cell division was ectopically induced (Figure 5c,f).

To explore this interaction, we employed cell-type-specific promoters to target differentiating cells, specifically rhizoid precursors and oil body cells (Sauret-Gueto et al., 2020; Romani et al., 2024). Both cell types, identifiable by their reduced chlorophyll content and distinct morphology, showed specific expression of Mp*CYCD;1* at the gemma stage. Misexpression of Mp*CYCD;1* under a rhizoid specific promoter (*pro*MpRSL3) caused ectopic cell divisions, resulting in the eventual loss of rhizoids (Figure 6c). Similarly, misexpression in oil body cells (*pro*MpERF13) triggered ectopic divisions, leaving smaller, scattered oil body cells in the gemma (Figure 6). Notably, these effects were not observed in Mp*CYCB;1* misexpression lines (Suppl. Figure 8).

During regeneration, both rhizoid precursors and oil body cells can undergo division and regenerate an entire plant after cell reprogramming (Nagai, 1919; Romani et al., 2024). De-differentiation of rhizoid precursors into epidermal cells is a normal phenomenon in some dorsal but not in ventral rhizoid precursors (Romani et al., 2024). The misexpression of Mp*CYCD;1* appears to extend this phenomenon, promoting widespread de-differentiation across ventral and dorsal precursors, impacting the emergence of rhizoids.

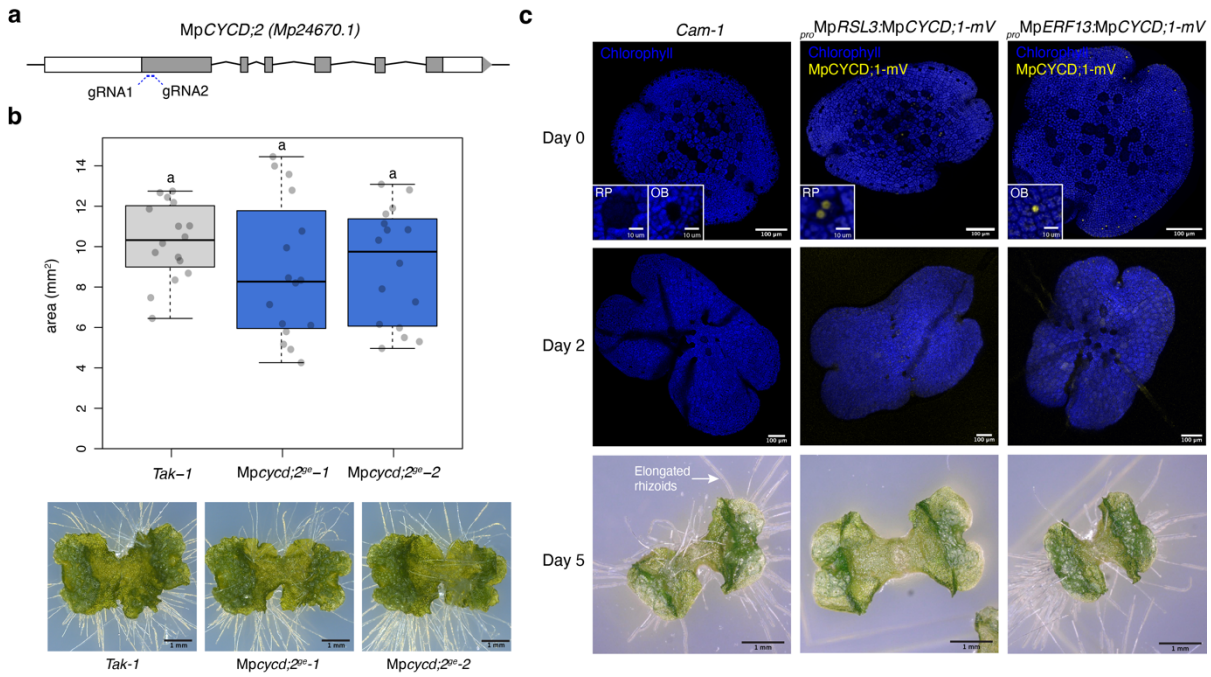

Figure 6.* Mp*CYCD;2* *knock-out and cell-type specific overexpression of* Mp*CYCD;1* *using cell-types specific promoters. a) Structure of MpCYCD;2 locus with the position of designed guide RNA (gRNA). Exons are shown as boxes. b)

433 *Boxplot of plant area of Mpcycd;2^{ge} and wild-type plants (Tak-1). Representative*
434 *pictures of the plants are shown at the bottom.* Scale bar lengths are indicated in the
435 pictures. Symbols above the bars indicate grouping by P-value<0.001 in a Tukey's
436 Honest Significant Difference method. c) Plants expressing *pro*Mp*RSL3*:Mp*CYCD;1-*
437 *mVenus (rhizoid precursor specific) and* *pro*Mp*ERF13*:Mp*CYCD;1-mVenus (oil body*
438 *specific). Wild-type Cam-1 was used as a control. Confocal full-stack images of*
439 *representative individual gemmalings (0, and 3) are shown with mVenus (yellow) and*
440 *chlorophyll (blue) channels merged. Representative picture of 5-days old gemmalings.*
441 Scale bar lengths are indicated in the pictures. *RP: rhizoid precursors. OB: oil bodies.*

442

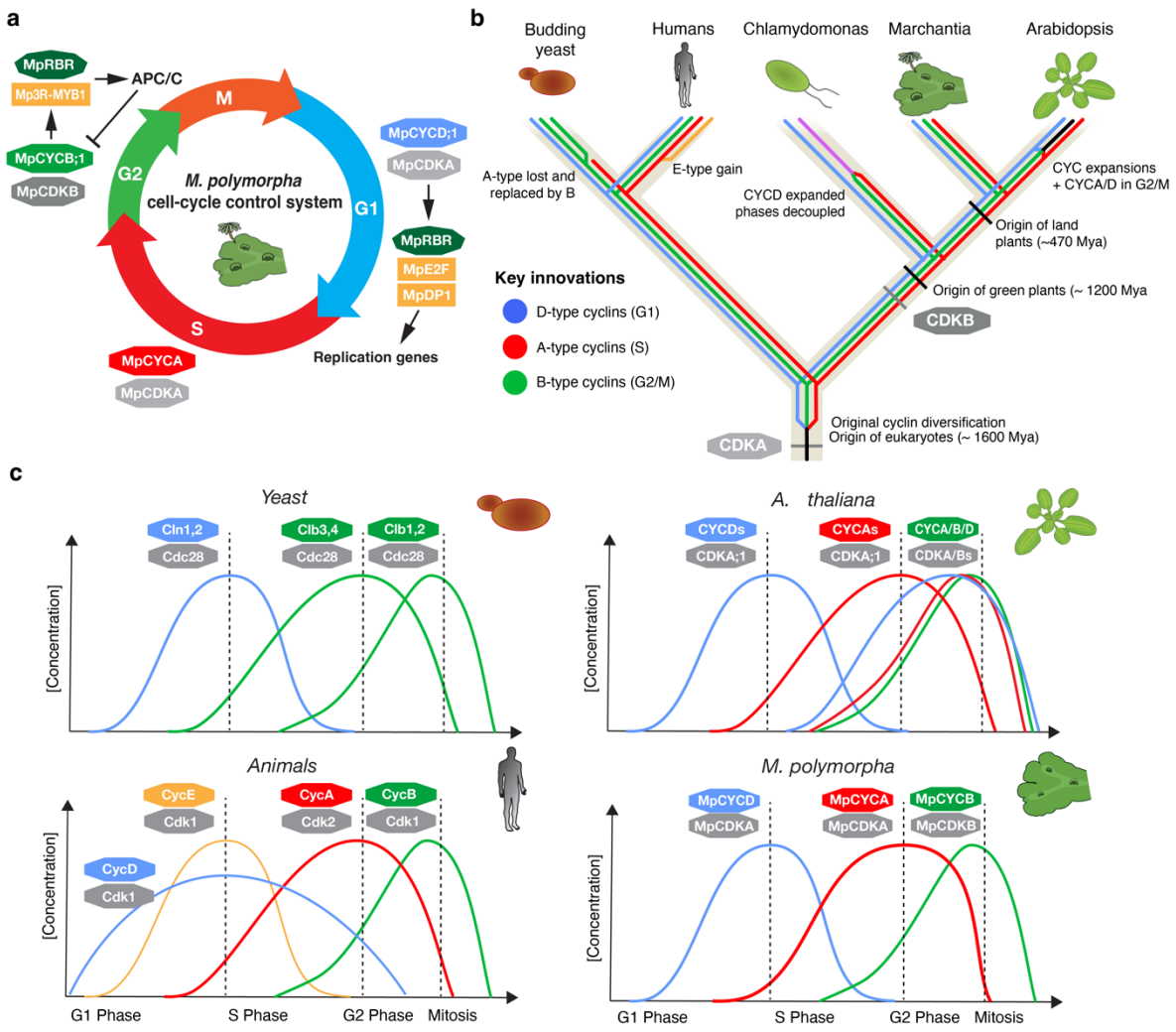

443

444 ***Figure 7. Core regulatory network of the cell cycle and phase specificity in***
445 ***Marchantia and other species****. a) Diagram of cell cycle control system in Marchantia.*
446 *b) Phylogram of the evolutionary trajectory of cell cycle genes in model eukaryotes*

447 *(Saccharomyces cerevisiae, Homo sapiens, C. reinhartii, A. thaliana, and M.*
448 *polymorpha) and its possible ancestral state. c) Comparison of expression patterns of*
449 *cyclins and CDKs.*

450

451 **DISCUSSION**

452 We systematically characterised for the first time the functional integration of core cell-
453 cycle genes in Marchantia. The genetic simplicity of Marchantia is second to none
454 among plant model organisms, as its cell-cycle control system is neither expanded (as
455 in most eukaryotes) nor reduced (as in yeast). On the other hand, displays the main
456 features conserved among plants and has the potential to bridge the gap between
457 unicellular algae and flowering plants at the systems level.

458 We showed that Marchantia displays simple set of cell-cycle genes (Figure 1).
459 Particularly, the expression of cyclins follows an archetypal pattern with each gene
460 peaking at the corresponding phase of its putative function, resembling the cell cycle
461 regulation observed in animals and yeast. To achieve this, cyclin expression is tightly
462 controlled at the transcriptional (Figure 2) and posttranscriptional (Figure 3) levels. In
463 Marchantia this pattern is characterized by CYCD and CDKA during G1-phase, CYCA
464 during S-phase, and CYCB and CDKB in G2/M (Figure 7a). Based on phylogenetic
465 analysis and functional studies in Marchantia and other species, it can be inferred that
466 this simple configuration represents the ancestral state of cell cycle regulation in
467 eukaryotes, except for CDKB being specific to plants (Figure 7b).

468 The streamlined system of cyclin-CDK components in Marchantia indicates that a
469 complex regulatory network is not a prerequisite for multicellularity in plants but rather
470 a derived feature in flowering plants. Thus, the extensive cyclin diversity observed in
471 vascular plants likely arose through lineage-specific gene duplications, leading to
472 redundancy and diversification. Subsequent neofunctionalization and
473 subfunctionalization, may have facilitated cellular innovations and tissue specificity. In
474 contrast, the set of key regulators that we described here for Marchantia are expressed
475 in both the haploid and diploid generation (Suppl. Figure 1). This might imply that a
476 very similar machinery controls cell division across both generations and meiosis, with
477 few specific features.

478 The only two gene duplications among Class I cyclins in Marchantia, Mp*CYCB;2* and
479 Mp*CYCD;2,* do not appear be relevant for cell cycle regulation. Mp*CYCB;2* is likely a
480 pseudogene with negligible expression, while Mp*CYCD;2* belonging to a bryophyte-
481 specific clade (CycD'). Overexpression, subcellular localization. and mutant
482 phenotypes suggest that Mp*CYCD;2* is not a canonical D-type cyclin, and it is
483 dispensable for vegetative growth.

484 Determining the truly essential components for the cell cycle progression remains a
485 challenge across eukaryotes. While CDKA plays a central role across eukaryotes, it is
486 not strictly essential in *Arabidopsis, Physcomitrium, and Chlamydomonas* (Nowack et
487 al., 2012; Tulin and Cross, 2015; Bao et al., 2022). In Marchantia, CDKA is steadily
488 expressed in dividing cells, with some preference for G1 (Figure 3), and does not
489 appear to be a rate-limiting factor (Figure 5). CDKB, a G2/M-specific innovation
490 conserved across green plants, is essential for spindle formation and nuclear division
491 in *Chlamydomonas* (Tulin and Cross, 2014; Pecani et al., 2022). Our results suggest
492 that MpCDKB is highly expressed at G2/M, likely interacting with MpCYCB;1.
493 However, CDK protein levels are detected throughout the cell cycle and do not exhibit
494 the strict phase-specific posttranscriptional regulation observed for cyclins.

495 D-type cyclins are conserved across eukaryotes and are undoubtedly important for
496 plant growth and development, though their essentiality in plants remains unclear
497 (Cross and Umen, 2015). Overexpression of Mp*CYCD;1* in Marchantia produces
498 phenotypes similar to those observed for *CYCD3* homologs in flowering plants
499 (Dewitte et al., 2003; Koroleva et al., 2004; Menges et al., 2006), reinforcing the idea
500 that regulating cell cycle re-entry is the ancestral role of D-type cyclins in plants. This
501 is important to understand the divergent roles of other D-type cyclins in flowering
502 plants, and contrast with the role of D-type cyclins in animals (Datar et al., 2000).

503 We also demonstrated a close relationship between cyclin-mediated cell cycle re-entry
504 and cellular differentiation in Marchantia (Figure 6). Our findings suggest that
505 maintaining proper coordination of cell division rates is essential for preserving cell
506 identity. This contrasts with Arabidopsis, where manipulating the cell cycle in
507 specialized cells, such as trichomes, alters cell size and induces multicellularity but
508 maintain cell identity (Schnittger et al., 2002b; Schnittger et al., 2002a). These

509 differences may help explain Marchantia's remarkable regenerative capacity and
510 developmental plasticity (Nishihama et al., 2015).

511 Interestingly, overexpression of Mp*CYCA* or Mp*CYCB* is deleterious in Marchantia,
512 leading to cell cycle arrest. In the case of A-type cyclins, they are usually associated
513 with ploidy level and control of S-phase duration in plants (Imai et al., 2006). However,
514 this might not be the case in Marchantia and other non-seed plants due to the absence
515 of endoreduplication (Bainard et al., 2013; Nishihama et al., 2015). In
516 *Chlamydomonas*, CYCA plays a critical role in cell division, but it is not essential
517 (Atkins and Cross, 2018). It was also shown that overexpression of *CYCA3* in
518 Arabidopsis cyclins affect meristem activity (Takahashi et al., 2010; Willems et al.,
519 2020). Given that Arabidopsis *CYCA3* cyclins are also expressed at the S phase as
520 MpCYCA in Marchantia. This suggest that controlling cell cycle progression during the
521 S phase could be the ancestral role for A-type cyclins across plants. Subsequently,
522 the role in ploidy could be restricted to the *CYCA2* clade and meiosis to *CYCA1* clade
523 (d'Erfurth et al., 2010).

524 In the case of B-type cyclins, both function and phase specificity are well conserved
525 across eukaryotes, playing a key role in regulating the G2/M transition, as we showed
526 in Marchantia. Their essentiality for cell division was demonstrated in *Chlamydomonas*
527 (Pecani et al., 2022). Historically, overexpression of *CYCB* is often associated with
528 higher division rates (Doerner et al., 1996). However, in Marchantia, overexpression
529 of Mp*CYCB;1* or Mp*CYCA* did not increase division rates but instead caused mitotic
530 arrest. This arrest may result from the inability of some cells to degrade excessive
531 cyclins, thereby preventing progression through mitosis (Figure 5h). The expression
532 of non-degradable CYCBs in plants and other eukaryotes has also been shown to
533 cause mitotic arrest, supporting that their degradation by the APC/C is critical (Figure
534 6). Similarly, A-type cyclins also need to be degraded by the APC/C but prior to the
535 spindle assembly checkpoint in other eukaryotes (Geley et al., 2001). Our results
536 suggest that *CYCA* degradation is also critical for cell-cycle progression in plants too
537 (Figure 5).

538 It remains an open question whether A- or B-type cyclins are limiting factors for growth
539 in Marchantia, as has been observed in other plants (Doerner et al., 1996). A possible

540 explanation is that the balance between cell division or arrest is highly dose
541 dependent. In addition to their role in mitotic control, CYCB1;1 induction in Arabidopsis
542 has also been shown to cause mitotic arrest under DNA damage conditions
543 (Schnittger and De Veylder, 2018). In animals, B-type cyclins are also not rate limiting
544 for cell proliferation (Doonan and Hunt, 1996), suggesting that this could represent the
545 ancestral state of CYCB protein function in eukaryotes. However, further studies are
546 required to generalize the precise functions of A- and B-type cyclins in plants.

547 On the other hand, we showed that MpCYCD;1 is the single rate-limiting cyclin/CDK
548 component for cell proliferation in Marchantia. Unlike MpCYCA and MpCYCB;1, its
549 degradation may not be required for mitotic progression. Rather, its accumulation
550 triggers re-entry into G1 and may be crucial for integrating developmental and
551 environmental signals to regulate plant growth rate.

552 The role of the DREAM complex TFs (E2F/DP and 3R-MYBs) is also important to
553 shape the downstream signalling networks of the cell cycle. The Marchantia genome
554 encodes homologs of these regulators, but only one copy of each component is
555 expressed in the gametophyte. The single-copy nature of E2F TFs in Marchantia and
556 other land plants suggests that the complexity observed in Arabidopsis and animals
557 arose independently (Sozzani et al., 2006; Rauber et al., 2016). The diversification of
558 3R-MYBs appears to be ancestral to land plants, and their expansion in Marchantia
559 may be linked to sporophyte-specific programs (Supplementary File 1).

560 In conclusion, Marchantia provides a valuable model for studying cell cycle to
561 demonstrate general principles of growth regulation that could be applied to complex
562 organisms. Further studies using conditional knockouts (Nishihama et al., 2016) could
563 clarify the roles of specific cell cycle genes in land plants. Additionally, targeted
564 investigations into how environmental stress, DNA damage, hormones, or mechanical
565 cues influence cell cycle progression will further enhance our understanding. The
566 foundational work presented here establishes a toolkit of genes and promoters that
567 can be leveraged for biotechnological applications. A deeper understanding of the cell
568 cycle will enable more precise approaches to reprogramming plant growth and
569 development.

570

ACKNOWLEDGEMENTS

This work was funded by BBSRC BB/T007117/1 to J.H, BBSRC BB/F011458/1 for confocal microscopy, JSPS KAKENHI Grant Number JP22H02676 to Y.H., and Takeda Science Foundation (Life Science Research Grants, 2024034869) to Y.H. F.R. is a Leverhulme Early Career Fellow (ECF-2023-534) funded by the Leverhulme Trust and the Isaac Newton Trust (23.08(f)), I.B. is funded by the Herschel Smith Fund studentship. We thank Miguel A. Blazquez and Antonio Serrano Mislata (IBMCP, Valencia, Spain) for useful discussion and feedback on the manuscript. We thank Jia-Wei Wang and Long Wang (CAS, China) for advice and help on scRNA-seq data analysis.

582 **MATERIAL AND METHODS**

583 **Phylogenetic analysis**

584 *Ceratopteris richardii* v2.1 (Marchant et al., 2022), *Amborella trichopoda* v1.0
585 (Amborella Genome, 2013), *Chlamydomonas reinhardtii* v5.5 (Merchant et al., 2007),
586 *Physcomitrium patens* v6.1 (Bi et al., 2024) and *Spirodela polyrhiza v2* (Wang et al.,
587 2014) proteomes were obtained from Phytozome. *Phaeodactylum tricornutum*
588 ASM15095 v2 (Bowler et al., 2008), *Prasinoderma coloniale* v1.1 (Li et al., 2020b),
589 *Ostreococcus lucimarinus* ASM9206 v1 (Palenik et al., 2007), *Mesotaenium*
590 *endlicherianum* v2 (Cheng et al., 2019), *Mesostigma viridea* (Liang et al., 2020)(ref),
591 *Ectocarpus siliculosus (Cock et al., 2010)*, and *Chara braunii* v1.0 (Nishiyama et al.,
592 2018) proteomes were obtained from Phycocosm. *Saccharomyces cerevisiae* R64.1.1
593 (Goffeau et al., 1996), *Caenorhabditis elegans (Consortium, 1998)*, and *Drosophila*
594 *melanogaster* BDGP6.46 (Adams et al., 2000) proteomes were obtained from
595 Ensembl, and *Cyanidioschyzon merolae* ASM9120 v1 (Matsuzaki et al., 2004) was
596 obtained from Ensembl Plants. The proteomes from *Marchantia polymorpha Tak* v6.1
597 (Montgomery et al., 2020), *Selaginella kraussiana* v2 (Liu et al., 2023), *Anthoceros*
598 *agresti* Oxford (Li et al., 2020a), *Klebsormidium nitens* NIES-2285 (Hori et al., 2014),
599 *Zygnema circumcarinatum* (Feng et al., 2024), *Penium margaritaceum* (Jiao et al.,
600 2020), *Marchantia paleacea* (Radhakrishnan et al., 2020), *Lunularia cruciata* v1 (Linde
601 et al., 2020) from their respective sources.

602 Hidden Markov Models matrix for PFAMs including cyclins (PF00134.28), CKS
603 (PF01111.24), E2F (PF02319.25), and RBR (PF01858.22) were used as query for
604 searching using hmmsearch function from HMMER v3.4 (Finn et al., 2011). The cut-
605 off E-value was then adjusted aiming to have 100% sensitivity for annotated genes
606 and exclude low confidence findings: Cyclins < 1E-10, CKS < 1E-10, E2F < 1E-5, RBR
607 < 1E-50. Using the hmmsearch output, Seqinr in R (Charif and Lobry, 2007) package
608 was to retrieve the sequences from the proteomes.

609 3R-MYBs proteins were BLASTed using the human MYBB sequence as a query
610 (threshold E-value < 2e-34) aiming to have 100% sensitivity for annotated 3R-MYB
611 and include some R2R3-MYBs. Similarly, for CDK proteins, using yeast CDC28 and
612 Arabidopsis CDKF as query (threshold E-value < 1e-44) aiming to have 100%

613 sensitivity for annotated CDKs. Sequences were extracted from the proteomes using
614 Biostrings package in R (Lifschitz et al., 2022).

615 Finally, JalView (Procter et al., 2021) was used to align sequences with the MAFFT
616 software (Katoh et al., 2002) and trimming the alignment to include only columns with
617 50% coverage. Maximum-likelyhood phylogenetic analysis was performed using
618 IQtree 2 (Minh et al., 2020) with default parameters. Trees were rooted and visualised
619 using iTOL v6 (Letunic and Bork, 2024). Complete trees available at (Suppl. File 1).

620 To count the number of MYB repeats (SM00717) for 3R-MYB proteins, we used
621 InterProScan (Quevillon et al., 2005). To identify signature motifs on CDKs we used a
622 simple grepl search function. Marchantia genes names were annotated in
623 MarpolBase.

624

625 **Analysis of public RNA-sequencing data**

626 TPM values for sporeling germination and different developmental stages were
627 extracted from Marpolbase Expression database (Kawamura et al., 2022) or
628 downloaded from SRA for regeneration (DRR330148- DRR330173), mapped in *M.*
629 *polymorpha* Tak-1 genome v5.1 using HISAT2 (Kim et al., 2019), ht-seq and EdgeR.
630 Data was subsequently analysed with R to generate plots using customs scripts.
631 Heatmap was generated using Marpolbase Expression database (Kawamura et al.,
632 2022).

633 The scRNA-seq matrix for Marchantia gemmaling development (Wang et al., 2023)
634 was extracted from Beijing Institute of Genomics Data Center (OMIX004749) and re-
635 analysed using Seurat V5 package in R (Hao et al., 2024). Briefly, the dataset was
636 subseted to only cluster 10 and analysed with the following functions and parameters:
637 FindNeighbours (dims = 1:100, k.param = 200), FindClusters, RunUMAP (reduction =
638 'pca', metric = 'correlation', n.neighbours = 30L, dims = 1:100). Data was visualized
639 using DimPlot, FeaturePlot and DotPlot functions. Markers in Suppl. Table S1 was
640 obtained using FindAllMarkers function and genes annotated using MarpolBase.

641

642 **Plant material and growth conditions**

643 *Marchantia polymorpha* subs*. rudelaris* accessions *Cam-1* (male) and *Cam-2* (female)
644 were used for most of the experiments. Under normal conditions, plants were grown
645 on solid 0.5× Gamborg B-5 basal medium (Phytotech #G398) at pH 5.8 with 1.2%
646 (w/v) agar micropropagation grade (Phytotech #A296), under continuous LED light at
647 21 °C with light intensity of 150 μmol/m^2/s (Systion #SE-EGB). For spore production,
648 plants were grown in Microbox micropropagation containers ($SacO_2$) in long-day
649 conditions (16 h light/8 h dark) under light supplemented with far-red light as described
650 (Sauret-Gueto et al., 2020).

651 For Mp*cycd;2* knock-outs, the *M. polymorpha* subs*. rudelaris* male accession
652 Takaragaike-1 (Tak-1) accession was used as wild type. Similarly, *M. polymorpha*
653 plants were grown on half-strength Gamborg B5 medium (pH 5.5) solidified with 1.4%
654 (w/v) agar at 22 °C under continuous light.

655

656 **Plasmid construction**

657 To generate new L0 parts, CDS and promoter regions from genes were extracted from
658 *M. polymorpha* Tak-1 genome version 5.1 (Bowman et al., 2017) genome and
659 manually domesticated to remove internal BsaI and SapI sites using synonymous
660 mutations for the CDS. The sequences of synthetic L0 parts used in this work are
661 available in Suppl. Table S2. L0 parts were synthesized by GENEWIZ following the
662 standard syntax for plant synthetic biology with CDS and PROM5 or PROM and 5UTR
663 overhangs and cloned into the plasmid pUAP1 (Addgene #63674) (Patron et al., 2015)
664 by homology recombination. Other parts were derived from previous works (Sauret-
665 Gueto et al., 2020; Romani et al., 2024) as specified in Suppl. Table S2.

666 The acceptor pBy01 (Romani et al., 2024) was used to assemble using L0
667 corresponding to PROM5 or PROM and 5UTR parts and pBy10 (Tse et al., 2024) for
668 entire cassettes containing a hygromycin resistant cassette for plant selection. These
669 acceptors are binary vectors contain a LacZ selection cassette flanked by BsaI sites
670 to clone final vectors in one-step using L0 parts following the standard syntaxis (Patron
671 et al., 2015). Following the same logic, a new custom acceptor for chlorosulfuron
672 selection was generated based on pBy10 and OP-62 (Sauret-Gueto et al., 2020;
673 Romani et al., 2024). Another two custom acceptors were generated for cloning only

674 CDS with the $_{pro}$*35S* (pBy12) or estradiol inducible system using $_{pro}$*MpE2F:XVE* driving
675 the expression of $_{pro}$*LexA,* similar to previous published Gateway acceptor
676 pMpGWB168 *(Ishida et al., 2022)* and a $_{3utr}$*NOS* terminator, containing also an
677 hygromycin (pBy13) or chlorosulfuron (pBy23) resistant cassette for plant selection.
678 The full-length of the final constructs were verified by sequencing using the Oxford
679 Nanopore technology (Plasmidsaurus Inc.). The final plasmid map is provided in the
680 supplementary data (Supplemental File 2-3).

681 Plasmids were assembled as detailed in Suppl. Table S2 using Type-IIS cloning as
682 described previously for L3 plasmids (Romani et al., 2024). Briefly using a Master Mix
683 containing 10% (v/v) 10× T4 DNA ligase buffer (NEB #M0202), 5% (v/v) T4 DNA ligase
684 at 400 U/µL (NEB #M0202), 5% (v/v) BsaI at 20 U/µL (NEB #R3733), 10% (v/v)
685 acceptor at 40 ng/µL, 20% (v/v) pre-mixed L0 parts (~100 ng/µL) and water to a final
686 volume of 5 µL. Cycling conditions were 26 cycles of 37 °C for 3 min and 16 °C for 4
687 min. Termination and enzyme denaturation: 50 °C for 5 min, and 80 °C for 10 min.
688 Other L1 and L2 plasmids were cloned as described before (Sauret-Gueto et al.,
689 2020). TOP10 chemically competent *Escherichia coli* cells were transformed using the
690 assembly reaction and plated on LB-agar plates containing the corresponding
691 antibiotic and 40 µg/mL of 5-bromo-4-chloro-3-indolyl β-D-galactopyranoside (X-Gal).
692 The presence of the correct insert was confirmed by restriction XhoI digestion (Thermo
693 Scientific #FD0694) and Sanger sequencing, with primers available at Supplemental
694 Table S2.

695 For genome editing of Mp*CYCD;2* (*Mp1g24670*), guide RNA was designed at the
696 coding sequence of the first intron using CRISPRdirect (Naito et al., 2015) and primers
697 at Supplemental Table S2. The plasmids were constructed according to Sugano et al.,
698 using pMpGE_En03 and pMpGE010 (Sugano et al., 2018).

699

700 **Plant transformation**

701 *Agrobacterium tumefaciens* (GV3101) cells were transformed using the freeze-thaw
702 method and used for plant transformation of *Cam-1/2* spores as described in Annese
703 et al., (2025). Plants were screened for positive fluorescence and at least two
704 independent lines were selected. For expression markers, representative transgenic

705 lines are shown, showing the consensus expression pattern out of 4-5 independent
706 lines.

707 For genome editing of Mp*CYCD;2*, Tak-1 plants were transformed using the cutting
708 thallus transformation protocol (Kubota et al., 2013) and genotyped using primers at
709 Supplemental Table S2.

710

711 **Plant phenotyping**

712 Representative images of Marchantia plants were taken using a Keyence VHX-5000
713 digital microscope equipped with a 20x-200x Ultra-Small, High-Performance Zoom
714 Lens (VH-Z20R/Z20T) or a Leica DMS1000 digital microscope. Thallus area was
715 quantified from pictures (normally 7-days old gemmalings) with ImageJ software with
716 at least 10 biological replicates. Cell sizes were quantified from manual
717 segmentation of cells in 200x pictures using ImageJ. Only cells surrounding the
718 DDCZ but excluding smaller cells closer to the apical meristem. At least 50 cells
719 were measured for each biological replicate in at least 3 biological replicates.

720 For β-estradiol (#E8875, Merck) treatments, a 50 mM stock was dissolved in DMSO
721 and added to melted agar-Gamborg B-5 media at a final concentration of 5 μM as
722 described in Ishida et al., (2021). Plants were grown in microscopy contact plates
723 and visualized after 3 or 10 days in normal growth conditions.

724

725 **Laser scanning confocal microscopy**

726 Confocal images of Marchantia were acquired on a Leica SP8X spectral confocal
727 microscope upright system equipped with a 460 to 670 nm super continuum white light
728 laser (80% laser power), two CW laser lines 405, and 442 nm, and 5 Channel Spectral
729 Scanhead (four hybrid detectors and one photomultiplier). For slides, imaging was
730 conducted using either a 10× air objective (HC PL APO 10×/0.40 CS2) or a 20× air
731 objective (HC PL APO 20×/0.75 CS2). When observing fluorescent protein with
732 overlapping emission spectra, sequential scanning mode was selected. Excitation
733 laser wavelength and captured emitted fluorescence wavelength window were: for

734 mVenus (514 nm, 527 to 552 nm), and for chlorophyll autofluorescence (633, 687 to
735 739 nm).

736

737 **Time-course and time-lapses**

738 When imaging time-courses, plants grown under normal culture conditions in small
739 petri dishes, removed the lid for imaging, and returned the plants to the growth
740 chamber and imaged as described above. For live imaging, six stacked Gene Frames
741 (#AB0578, ThermoFisher) were placed on a glass slide and filled halfway with molten
742 Gamborg B-5 agar medium. Plants were then placed on the solidified agar surface
743 and meristems were removed using a Laser Microdissection Leica LMD7000.
744 Samples were mounted in perfluorodecalin (Littlejohn et al., 2010) with a glass
745 coverslip on top. The slides were then continuously imaged on the Leica SP8X
746 confocal microscope for 1 to 4 d.

747

748 **EdU staining**

749 5-days old gemmalings were incubated in liquid half-strength Gamborg's B-5 medium
750 under continuous light for 3 h with 20 µM 5-ethynyl- 2'-deoxyuridine (EdU) from the
751 Click-iT EdU Imaging Kit with Alexa Fluor 488 (#C10337, Invitrogen). Then they were
752 fixed with 4% formaldehyde for 1 h, washed twice with phosphate buffer saline (PBS)
753 and 0.5% Triton X-100 in PBS for 20 min. After washes, samples were incubated with
754 a freshly prepared reaction mixture following the manufacturer instructions but without
755 the Hoechst 33342 component. After staining, samples were protected from light,
756 washed twice with PBS and soaked in iTomei-D (#T3940, Tokyo Chemical Industry)
757 clearing solution and mounted in 70% w/v iohexol (#I0903, Tokyo Chemical Industry)
758 in PBS as described before (Sakamoto et al., 2022). Samples were covered with a
759 glass coverslip and imaged on the Leica SP8X confocal microscope as described
760 before.

761

762 **Statistics**

To obtain plots and statistical analysis, data was processed using R xv 4.4.1 software. For average and boxplots, the stats package was used with default parameters. For violinplots, the vioplot package was implemented also with default parameters. Statistical significance was calculated using ANOVA using the stats package Tukey 'Honest Significant Difference' method (alpha = 0.05) for levels calculations.

REFERENCES

Adams, M.D., Celniker, S.E., Holt, R.A., Evans, C.A., Gocayne, J.D., Amanatides, P.G., Scherer, S.E., Li, P.W., Hoskins, R.A., Galle, R.F., George, R.A., Lewis, S.E., Richards, S., Ashburner, M., Henderson, S.N., Sutton, G.G., Wortman, J.R., Yandell, M.D., Zhang, Q., Chen, L.X., Brandon, R.C., Rogers, Y.H., Blazej, R.G., Champe, M., Pfeiffer, B.D., Wan, K.H., Doyle, C., Baxter, E.G., Helt, G., Nelson, C.R., Gabor, G.L., Abril, J.F., Agbayani, A., An, H.J., Andrews-Pfannkoch, C., Baldwin, D., Ballew, R.M., Basu, A., Baxendale, J., Bayraktaroglu, L., Beasley, E.M., Beeson, K.Y., Benos, P.V., Berman, B.P., Bhandari, D., Bolshakov, S., Borkova, D., Botchan, M.R., Bouck, J., Brokstein, P., Brottier, P., Burtis, K.C., Busam, D.A., Butler, H., Cadieu, E., Center, A., Chandra, I., Cherry, J.M., Cawley, S., Dahlke, C., Davenport, L.B., Davies, P., de Pablos, B., Delcher, A., Deng, Z., Mays, A.D., Dew, I., Dietz, S.M., Dodson, K., Doup, L.E., Downes, M., Dugan-Rocha, S., Dunkov, B.C., Dunn, P., Durbin, K.J., Evangelista, C.C., Ferraz, C., Ferriera, S., Fleischmann, W., Fosler, C., Gabrielian, A.E., Garg, N.S., Gelbart, W.M., Glasser, K., Glodek, A., Gong, F., Gorrell, J.H., Gu, Z., Guan, P., Harris, M., Harris, N.L., Harvey, D., Heiman, T.J., Hernandez, J.R., Houck, J., Hostin, D., Houston, K.A., Howland, T.J., Wei, M.H., Ibegwam, C., Jalali, M., Kalush, F., Karpen, G.H., Ke, Z., Kennison, J.A., Ketchum, K.A., Kimmel, B.E., Kodira, C.D., Kraft, C., Kravitz, S., Kulp, D., Lai, Z., Lasko, P., Lei, Y., Levitsky, A.A., Li, J., Li, Z., Liang, Y., Lin, X., Liu, X., Mattei, B., McIntosh, T.C., McLeod, M.P., McPherson, D., Merkulov, G., Milshina, N.V., Mobarry, C., Morris, J., Moshrefi, A., Mount, S.M., Moy, M., Murphy, B., Murphy, L., Muzny, D.M., Nelson, D.L., Nelson, D.R., Nelson, K.A., Nixon, K., Nusskern, D.R., Pacleb, J.M., Palazzolo, M., Pittman, G.S., Pan, S., Pollard, J., Puri, V., Reese, M.G., Reinert, K., Remington, K., Saunders, R.D., Scheeler, F., Shen, H., Shue, B.C., Siden-Kiamos, I., Simpson, M., Skupski, M.P., Smith, T., Spier, E., Spradling, A.C., Stapleton, M., Strong, R., Sun, E., Svirskas, R., Tector, C., Turner, R., Venter, E., Wang, A.H., Wang, X., Wang, Z.Y., Wassarman, D.A., Weinstock, G.M., Weissenbach, J., Williams, S.M., WoodageT, Worley, K.C., Wu, D., Yang, S., Yao, Q.A., Ye, J., Yeh, R.F., Zaveri, J.S., Zhan, M., Zhang, G., Zhao, Q., Zheng, L., Zheng, X.H., Zhong, F.N., Zhong, W., Zhou, X., Zhu, S., Zhu, X., Smith, H.O., Gibbs, R.A., Myers, E.W., Rubin, G.M., and Venter, J.C. (2000). The genome sequence of Drosophila melanogaster. Science **287,** 2185-2195.

Amborella Genome, P. (2013). The Amborella genome and the evolution of flowering plants. Science **342,** 1241089.

806 **Atkins, K.C., and Cross, F.R.** (2018). Interregulation of CDKA/CDK1 and the Plant-
807 Specific Cyclin-Dependent Kinase CDKB in Control of the Chlamydomonas Cell
808 Cycle. Plant Cell **30,** 429-446.
809 **Attrill, S.T., Mulvey, H., Champion, C., and Dolan, L.** (2024). Microtubules and actin
810 filaments direct nuclear movement during the polarisation of Marchantia spore
811 cells. Development **151**.
812 **Azumi, Y., Liu, D., Zhao, D., Li, W., Wang, G., Hu, Y., and Ma, H.** (2002). Homolog
813 interaction during meiotic prophase I in Arabidopsis requires the SOLO DANCERS
814 gene encoding a novel cyclin-like protein. EMBO J **21,** 3081-3095.
815 **Bainard, J.D., Forrest, L.L., Goffinet, B., and Newmaster, S.G.** (2013). Nuclear DNA
816 content variation and evolution in liverworts. Mol Phylogenet Evol **68,** 619-627.
817 **Bao, L., Inoue, N., Ishikawa, M., Gotoh, E., Teh, O.K., Higa, T., Morimoto, T., Ginanjar,**
818 **E.F., Harashima, H., Noda, N., Watahiki, M., Hiwatashi, Y., Sekine, M.,**
819 **Hasebe, M., Wada, M., and Fujita, T.** (2022). A PSTAIRE-type cyclin-dependent
820 kinase controls light responses in land plants. Sci Adv **8,** eabk2116.
821 **Bi, G., Zhao, S., Yao, J., Wang, H., Zhao, M., Sun, Y., Hou, X., Haas, F.B., Varshney, D.,**
822 **Prigge, M., Rensing, S.A., Jiao, Y., Ma, Y., Yan, J., and Dai, J.** (2024). Near
823 telomere-to-telomere genome of the model plant Physcomitrium patens. Nat
824 Plants **10,** 327-343.
825 **Boruc, J., Mylle, E., Duda, M., De Clercq, R., Rombauts, S., Geelen, D., Hilson, P.,**
826 **Inze, D., Van Damme, D., and Russinova, E.** (2010). Systematic localization of
827 the Arabidopsis core cell cycle proteins reveals novel cell division complexes.
828 Plant Physiol **152,** 553-565.
829 **Bowler, C., Allen, A.E., Badger, J.H., Grimwood, J., Jabbari, K., Kuo, A., Maheswari,**
830 **U., Martens, C., Maumus, F., Otillar, R.P., Rayko, E., Salamov, A., Vandepoele,**
831 **K., Beszteri, B., Gruber, A., Heijde, M., Katinka, M., Mock, T., Valentin, K.,**
832 **Verret, F., Berges, J.A., Brownlee, C., Cadoret, J.P., Chiovitti, A., Choi, C.J.,**
833 **Coesel, S., De Martino, A., Detter, J.C., Durkin, C., Falciatore, A., Fournet, J.,**
834 **Haruta, M., Huysman, M.J., Jenkins, B.D., Jiroutova, K., Jorgensen, R.E.,**
835 **Joubert, Y., Kaplan, A., Kroger, N., Kroth, P.G., La Roche, J., Lindquist, E.,**
836 **Lommer, M., Martin-Jezequel, V., Lopez, P.J., Lucas, S., Mangogna, M.,**
837 **McGinnis, K., Medlin, L.K., Montsant, A., Oudot-Le Secq, M.P., Napoli, C.,**
838 **Obornik, M., Parker, M.S., Petit, J.L., Porcel, B.M., Poulsen, N., Robison, M.,**
839 **Rychlewski, L., Rynearson, T.A., Schmutz, J., Shapiro, H., Siaut, M., Stanley,**
840 **M., Sussman, M.R., Taylor, A.R., Vardi, A., von Dassow, P., Vyverman, W.,**
841 **Willis, A., Wyrwicz, L.S., Rokhsar, D.S., Weissenbach, J., Armbrust, E.V.,**
842 **Green, B.R., Van de Peer, Y., and Grigoriev, I.V.** (2008). The Phaeodactylum
843 genome reveals the evolutionary history of diatom genomes. Nature **456,** 239-
844 244.
845 **Bowman, J.L., Arteaga-Vazquez, M., Berger, F., Briginshaw, L.N., Carella, P., Aguilar-**
846 **Cruz, A., Davies, K.M., Dierschke, T., Dolan, L., Dorantes-Acosta, A.E., Fisher,**
847 **T.J., Flores-Sandoval, E., Futagami, K., Ishizaki, K., Jibran, R., Kanazawa, T.,**
848 **Kato, H., Kohchi, T., Levins, J., Lin, S.S., Nakagami, H., Nishihama, R., Romani,**
849 **F., Schornack, S., Tanizawa, Y., Tsuzuki, M., Ueda, T., Watanabe, Y., Yamato,**
850 **K.T., and Zachgo, S.** (2022). The renaissance and enlightenment of Marchantia as
851 a model system. Plant Cell **34,** 3512-3542.

852 **Bowman, J.L., Kohchi, T., Yamato, K.T., Jenkins, J., Shu, S., Ishizaki, K., Yamaoka, S.,**
853 **Nishihama, R., Nakamura, Y., Berger, F., Adam, C., Aki, S.S., Althoff, F., Araki,**
854 **T., Arteaga-Vazquez, M.A., Balasubrmanian, S., Barry, K., Bauer, D., Boehm,**
855 **C.R., Briginshaw, L., Caballero-Perez, J., Catarino, B., Chen, F., Chiyoda, S.,**
856 **Chovatia, M., Davies, K.M., Delmans, M., Demura, T., Dierschke, T., Dolan, L.,**
857 **Dorantes-Acosta, A.E., Eklund, D.M., Florent, S.N., Flores-Sandoval, E.,**
858 **Fujiyama, A., Fukuzawa, H., Galik, B., Grimanelli, D., Grimwood, J.,**
859 **Grossniklaus, U., Hamada, T., Haseloff, J., Hetherington, A.J., Higo, A.,**
860 **Hirakawa, Y., Hundley, H.N., Ikeda, Y., Inoue, K., Inoue, S.I., Ishida, S., Jia, Q.,**
861 **Kakita, M., Kanazawa, T., Kawai, Y., Kawashima, T., Kennedy, M., Kinose, K.,**
862 **Kinoshita, T., Kohara, Y., Koide, E., Komatsu, K., Kopischke, S., Kubo, M.,**
863 **Kyozuka, J., Lagercrantz, U., Lin, S.S., Lindquist, E., Lipzen, A.M., Lu, C.W., De**
864 **Luna, E., Martienssen, R.A., Minamino, N., Mizutani, M., Mizutani, M.,**
865 **Mochizuki, N., Monte, I., Mosher, R., Nagasaki, H., Nakagami, H., Naramoto,**
866 **S., Nishitani, K., Ohtani, M., Okamoto, T., Okumura, M., Phillips, J., Pollak, B.,**
867 **Reinders, A., Rovekamp, M., Sano, R., Sawa, S., Schmid, M.W., Shirakawa, M.,**
868 **Solano, R., Spunde, A., Suetsugu, N., Sugano, S., Sugiyama, A., Sun, R.,**
869 **Suzuki, Y., Takenaka, M., Takezawa, D., Tomogane, H., Tsuzuki, M., Ueda, T.,**
870 **Umeda, M., Ward, J.M., Watanabe, Y., Yazaki, K., Yokoyama, R., Yoshitake, Y.,**
871 **Yotsui, I., Zachgo, S., and Schmutz, J.** (2017). Insights into Land Plant Evolution
872 Garnered from the Marchantia polymorpha Genome. Cell **171,** 287-304 e215.
873 **Breker, M., Lieberman, K., and Cross, F.R.** (2018). Comprehensive Discovery of Cell-
874 Cycle-Essential Pathways in Chlamydomonas reinhardtii. Plant Cell **30,** 1178-
875 1198.
876 **Brophy, J.A.N., LaRue, T., and Dinneny, J.R.** (2018). Understanding and engineering
877 plant form. Semin Cell Dev Biol **79,** 68-77.
878 **Charif, D., and Lobry, J.R.** (2007). SeqinR 1.0-2: A Contributed Package to the R Project
879 for Statistical Computing Devoted to Biological Sequences Retrieval and
880 Analysis. In Structural Approaches to Sequence Evolution: Molecules, Networks,
881 Populations, U. Bastolla, M. Porto, H.E. Roman, and M. Vendruscolo, eds (Berlin,
882 Heidelberg: Springer Berlin Heidelberg), pp. 207-232.
883 **Cheng, S., Xian, W., Fu, Y., Marin, B., Keller, J., Wu, T., Sun, W., Li, X., Xu, Y., Zhang,**
884 **Y., Wittek, S., Reder, T., Gunther, G., Gontcharov, A., Wang, S., Li, L., Liu, X.,**
885 **Wang, J., Yang, H., Xu, X., Delaux, P.M., Melkonian, B., Wong, G.K., and**
886 **Melkonian, M.** (2019). Genomes of Subaerial Zygnematophyceae Provide
887 Insights into Land Plant Evolution. Cell **179,** 1057-1067 e1014.
888 **Clute, P., and Pines, J.** (1999). Temporal and spatial control of cyclin B1 destruction in
889 metaphase. Nat Cell Biol **1,** 82-87.
890 **Cock, J.M., Sterck, L., Rouze, P., Scornet, D., Allen, A.E., Amoutzias, G., Anthouard,**
891 **V., Artiguenave, F., Aury, J.M., Badger, J.H., Beszteri, B., Billiau, K., Bonnet, E.,**
892 **Bothwell, J.H., Bowler, C., Boyen, C., Brownlee, C., Carrano, C.J., Charrier, B.,**
893 **Cho, G.Y., Coelho, S.M., Collen, J., Corre, E., Da Silva, C., Delage, L.,**
894 **Delaroque, N., Dittami, S.M., Doulbeau, S., Elias, M., Farnham, G., Gachon,**
895 **C.M., Gschloessl, B., Heesch, S., Jabbari, K., Jubin, C., Kawai, H., Kimura, K.,**
896 **Kloareg, B., Kupper, F.C., Lang, D., Le Bail, A., Leblanc, C., Lerouge, P., Lohr,**
897 **M., Lopez, P.J., Martens, C., Maumus, F., Michel, G., Miranda-Saavedra, D.,**
898 **Morales, J., Moreau, H., Motomura, T., Nagasato, C., Napoli, C.A., Nelson,**

D.R., Nyvall-Collen, P., Peters, A.F., Pommier, C., Potin, P., Poulain, J., Quesneville, H., Read, B., Rensing, S.A., Ritter, A., Rousvoal, S., Samanta, M., Samson, G., Schroeder, D.C., Segurens, B., Strittmatter, M., Tonon, T., Tregear, J.W., Valentin, K., von Dassow, P., Yamagishi, T., Van de Peer, Y., and Wincker, P. (2010). The Ectocarpus genome and the independent evolution of multicellularity in brown algae. Nature **465,** 617-621.

Consortium, C.e.S. (1998). Genome sequence of the nematode C. elegans: a platform for investigating biology. Science **282,** 2012-2018.

Cross, F.R. (2020). Regulation of Multiple Fission and Cell-Cycle-Dependent Gene Expression by CDKA1 and the Rb-E2F Pathway in Chlamydomonas. Curr Biol **30,** 1855-1865 e1854.

Cross, F.R., and Umen, J.G. (2015). The Chlamydomonas cell cycle. Plant J **82,** 370-392.

d'Erfurth, I., Cromer, L., Jolivet, S., Girard, C., Horlow, C., Sun, Y., To, J.P., Berchowitz, L.E., Copenhaver, G.P., and Mercier, R. (2010). The cyclin-A CYCA1;2/TAM is required for the meiosis I to meiosis II transition and cooperates with OSD1 for the prophase to first meiotic division transition. PLoS Genet **6,** e1000989.

Datar, S.A., Jacobs, H.W., de la Cruz, A.F., Lehner, C.F., and Edgar, B.A. (2000). The Drosophila cyclin D-Cdk4 complex promotes cellular growth. EMBO J **19,** 4543-4554.

Dewitte, W., Riou-Khamlichi, C., Scofield, S., Healy, J.M., Jacqmard, A., Kilby, N.J., and Murray, J.A. (2003). Altered cell cycle distribution, hyperplasia, and inhibited differentiation in Arabidopsis caused by the D-type cyclin CYCD3. Plant Cell **15,** 79-92.

Doerner, P., Jorgensen, J.E., You, R., Steppuhn, J., and Lamb, C. (1996). Control of root growth and development by cyclin expression. Nature **380,** 520-523.

Doonan, J., and Hunt, T. (1996). Cell cycle. Why don't plants get cancer? Nature **380,** 481-482.

Feng, G., Burleigh, J.G., Braun, E.L., Mei, W., and Barbazuk, W.B. (2017). Evolution of the 3R-MYB Gene Family in Plants. Genome Biol Evol **9,** 1013-1029.

Feng, X., Zheng, J., Irisarri, I., Yu, H., Zheng, B., Ali, Z., de Vries, S., Keller, J., Furst-Jansen, J.M.R., Dadras, A., Zegers, J.M.S., Rieseberg, T.P., Dhabalia Ashok, A., Darienko, T., Bierenbroodspot, M.J., Gramzow, L., Petroll, R., Haas, F.B., Fernandez-Pozo, N., Nousias, O., Li, T., Fitzek, E., Grayburn, W.S., Rittmeier, N., Permann, C., Rumpler, F., Archibald, J.M., Theissen, G., Mower, J.P., Lorenz, M., Buschmann, H., von Schwartzenberg, K., Boston, L., Hayes, R.D., Daum, C., Barry, K., Grigoriev, I.V., Wang, X., Li, F.W., Rensing, S.A., Ben Ari, J., Keren, N., Mosquna, A., Holzinger, A., Delaux, P.M., Zhang, C., Huang, J., Mutwil, M., de Vries, J., and Yin, Y. (2024). Genomes of multicellular algal sisters to land plants illuminate signaling network evolution. Nat Genet **56,** 1018-1031.

Finn, R.D., Clements, J., and Eddy, S.R. (2011). HMMER web server: interactive sequence similarity searching. Nucleic Acids Res **39,** W29-37.

Geley, S., Kramer, E., Gieffers, C., Gannon, J., Peters, J.M., and Hunt, T. (2001). Anaphase-promoting complex/cyclosome-dependent proteolysis of human cyclin A starts at the beginning of mitosis and is not subject to the spindle assembly checkpoint. J Cell Biol **153,** 137-148.

Goffeau, A., Barrell, B.G., Bussey, H., Davis, R.W., Dujon, B., Feldmann, H., Galibert, F., Hoheisel, J.D., Jacq, C., Johnston, M., Louis, E.J., Mewes, H.W., Murakami, Y., Philippsen, P., Tettelin, H., and Oliver, S.G. (1996). Life with 6000 genes. Science **274,** 546, 563-547.

Gutierrez, C. (2009). The Arabidopsis cell division cycle. Arabidopsis Book **7,** e0120.

Gutierrez, C. (2022). A Journey to the Core of the Plant Cell Cycle. Int J Mol Sci **23**.

Hao, Y., Stuart, T., Kowalski, M.H., Choudhary, S., Hoffman, P., Hartman, A., Srivastava, A., Molla, G., Madad, S., Fernandez-Granda, C., and Satija, R. (2024). Dictionary learning for integrative, multimodal and scalable single-cell analysis. Nat Biotechnol **42,** 293-304.

Hori, K., Maruyama, F., Fujisawa, T., Togashi, T., Yamamoto, N., Seo, M., Sato, S., Yamada, T., Mori, H., Tajima, N., Moriyama, T., Ikeuchi, M., Watanabe, M., Wada, H., Kobayashi, K., Saito, M., Masuda, T., Sasaki-Sekimoto, Y., Mashiguchi, K., Awai, K., Shimojima, M., Masuda, S., Iwai, M., Nobusawa, T., Narise, T., Kondo, S., Saito, H., Sato, R., Murakawa, M., Ihara, Y., Oshima-Yamada, Y., Ohtaka, K., Satoh, M., Sonobe, K., Ishii, M., Ohtani, R., Kanamori-Sato, M., Honoki, R., Miyazaki, D., Mochizuki, H., Umetsu, J., Higashi, K., Shibata, D., Kamiya, Y., Sato, N., Nakamura, Y., Tabata, S., Ida, S., Kurokawa, K., and Ohta, H. (2014). Klebsormidium flaccidum genome reveals primary factors for plant terrestrial adaptation. Nat Commun **5,** 3978.

Imai, K.K., Ohashi, Y., Tsuge, T., Yoshizumi, T., Matsui, M., Oka, A., and Aoyama, T. (2006). The A-type cyclin CYCA2;3 is a key regulator of ploidy levels in Arabidopsis endoreduplication. Plant Cell **18,** 382-396.

Inze, D., and De Veylder, L. (2006). Cell cycle regulation in plant development. Annu Rev Genet **40,** 77-105.

Ishida, S., Suzuki, H., Iwaki, A., Kawamura, S., Yamaoka, S., Kojima, M., Takebayashi, Y., Yamaguchi, K., Shigenobu, S., Sakakibara, H., Kohchi, T., and Nishihama, R. (2022). Diminished Auxin Signaling Triggers Cellular Reprogramming by Inducing a Regeneration Factor in the Liverwort Marchantia polymorpha. Plant Cell Physiol **63,** 384-400.

Ishikawa, M., Murata, T., Sato, Y., Nishiyama, T., Hiwatashi, Y., Imai, A., Kimura, M., Sugimoto, N., Akita, A., Oguri, Y., Friedman, W.E., Hasebe, M., and Kubo, M. (2011). Physcomitrella cyclin-dependent kinase A links cell cycle reactivation to other cellular changes during reprogramming of leaf cells. Plant Cell **23,** 2924-2938.

Ito, M., Araki, S., Matsunaga, S., Itoh, T., Nishihama, R., Machida, Y., Doonan, J.H., and Watanabe, A. (2001). G2/M-phase-specific transcription during the plant cell cycle is mediated by c-Myb-like transcription factors. Plant Cell **13,** 1891-1905.

Jiao, C., Sorensen, I., Sun, X., Sun, H., Behar, H., Alseekh, S., Philippe, G., Palacio Lopez, K., Sun, L., Reed, R., Jeon, S., Kiyonami, R., Zhang, S., Fernie, A.R., Brumer, H., Domozych, D.S., Fei, Z., and Rose, J.K.C. (2020). The Penium margaritaceum Genome: Hallmarks of the Origins of Land Plants. Cell **181,** 1097-1111 e1012.

Joubes, J., Chevalier, C., Dudits, D., Heberle-Bors, E., Inze, D., Umeda, M., and Renaudin, J.P. (2000). CDK-related protein kinases in plants. Plant Mol Biol **43,** 607-620.

991 **Katoh, K., Misawa, K., Kuma, K., and Miyata, T.** (2002). MAFFT: a novel method for rapid
992 multiple sequence alignment based on fast Fourier transform. Nucleic Acids Res
993 **30,** 3059-3066.
994 **Kawamura, S., Romani, F., Yagura, M., Mochizuki, T., Sakamoto, M., Yamaoka, S.,**
995 **Nishihama, R., Nakamura, Y., Yamato, K.T., Bowman, J.L., Kohchi, T., and**
996 **Tanizawa, Y.** (2022). MarpolBase Expression: A Web-Based, Comprehensive
997 Platform for Visualization and Analysis of Transcriptomes in the Liverwort
998 Marchantia polymorpha. Plant Cell Physiol **63,** 1745-1755.
999 **Kim, D., Paggi, J.M., Park, C., Bennett, C., and Salzberg, S.L.** (2019). Graph-based
1000 genome alignment and genotyping with HISAT2 and HISAT-genotype. Nat
1001 Biotechnol **37,** 907-915.
1002 **Kobayashi, K., Suzuki, T., Iwata, E., Magyar, Z., Bogre, L., and Ito, M.** (2015). MYB3Rs,
1003 plant homologs of Myb oncoproteins, control cell cycle-regulated transcription
1004 and form DREAM-like complexes. Transcription **6,** 106-111.
1005 **Komaki, S., and Sugimoto, K.** (2012). Control of the plant cell cycle by developmental
1006 and environmental cues. Plant Cell Physiol **53,** 953-964.
1007 **Koroleva, O.A., Tomlinson, M., Parinyapong, P., Sakvarelidze, L., Leader, D., Shaw,**
1008 **P., and Doonan, J.H.** (2004). CycD1, a putative G1 cyclin from Antirrhinum majus,
1009 accelerates the cell cycle in cultured tobacco BY-2 cells by enhancing both G1/S
1010 entry and progression through S and G2 phases. Plant Cell **16,** 2364-2379.
1011 **Krylov, D.M., Nasmyth, K., and Koonin, E.V.** (2003). Evolution of eukaryotic cell cycle
1012 regulation: stepwise addition of regulatory kinases and late advent of the CDKs.
1013 Curr Biol **13,** 173-177.
1014 **Kubota, A., Ishizaki, K., Hosaka, M., and Kohchi, T.** (2013). Efficient Agrobacterium-
1015 mediated transformation of the liverwort Marchantia polymorpha using
1016 regenerating thalli. Biosci Biotechnol Biochem **77,** 167-172.
1017 **Letunic, I., and Bork, P.** (2024). Interactive Tree of Life (iTOL) v6: recent updates to the
1018 phylogenetic tree display and annotation tool. Nucleic Acids Res **52,** W78-W82.
1019 **Li, F.W., Nishiyama, T., Waller, M., Frangedakis, E., Keller, J., Li, Z., Fernandez-Pozo,**
1020 **N., Barker, M.S., Bennett, T., Blazquez, M.A., Cheng, S., Cuming, A.C., de**
1021 **Vries, J., de Vries, S., Delaux, P.M., Diop, I.S., Harrison, C.J., Hauser, D.,**
1022 **Hernandez-Garcia, J., Kirbis, A., Meeks, J.C., Monte, I., Mutte, S.K., Neubauer,**
1023 **A., Quandt, D., Robison, T., Shimamura, M., Rensing, S.A., Villarreal, J.C.,**
1024 **Weijers, D., Wicke, S., Wong, G.K., Sakakibara, K., and Szovenyi, P.** (2020a).
1025 Anthoceros genomes illuminate the origin of land plants and the unique biology
1026 of hornworts. Nat Plants **6,** 259-272.
1027 **Li, L., Wang, S., Wang, H., Sahu, S.K., Marin, B., Li, H., Xu, Y., Liang, H., Li, Z., Cheng,**
1028 **S., Reder, T., Cebi, Z., Wittek, S., Petersen, M., Melkonian, B., Du, H., Yang, H.,**
1029 **Wang, J., Wong, G.K., Xu, X., Liu, X., Van de Peer, Y., Melkonian, M., and Liu,**
1030 **H.** (2020b). The genome of Prasinoderma coloniale unveils the existence of a third
1031 phylum within green plants. Nat Ecol Evol **4,** 1220-1231.
1032 **Liang, Z., Geng, Y., Ji, C., Du, H., Wong, C.E., Zhang, Q., Zhang, Y., Zhang, P., Riaz, A.,**
1033 **Chachar, S., Ding, Y., Wen, J., Wu, Y., Wang, M., Zheng, H., Wu, Y., Demko, V.,**
1034 **Shen, L., Han, X., Zhang, P., Gu, X., and Yu, H.** (2020). Mesostigma viride
1035 Genome and Transcriptome Provide Insights into the Origin and Evolution of
1036 Streptophyta. Adv Sci (Weinh) **7,** 1901850.

Lifschitz, S., Haeusler, E.H., Catanho, M., Miranda, A.B., Armas, E.M., Heine, A., Moreira, S., and Tristao, C. (2022). Bio-Strings: A Relational Database Data-Type for Dealing with Large Biosequences. BioTech (Basel) **11**.

Linde, A.M., Sawangproh, W., Cronberg, N., Szovenyi, P., and Lagercrantz, U. (2020). Evolutionary History of the Marchantia polymorpha Complex. Front Plant Sci **11,** 829.

Littlejohn, G.R., Gouveia, J.D., Edner, C., Smirnoff, N., and Love, J. (2010). Perfluorodecalin enhances in vivo confocal microscopy resolution of Arabidopsis thaliana mesophyll. New Phytol **186,** 1018-1025.

Liu, J., and Kipreos, E.T. (2000). Evolution of cyclin-dependent kinases (CDKs) and CDK-activating kinases (CAKs): differential conservation of CAKs in yeast and metazoa. Mol Biol Evol **17,** 1061-1074.

Liu, W., Cai, G., Zhai, N., Wang, H., Tang, T., Zhang, Y., Zhang, Z., Sun, L., Zhang, Y., Beeckman, T., and Xu, L. (2023). Genome and transcriptome of Selaginella kraussiana reveal evolution of root apical meristems in vascular plants. Curr Biol **33,** 4085-4097 e4085.

Ma, Z., Wu, Y., Jin, J., Yan, J., Kuang, S., Zhou, M., Zhang, Y., and Guo, A.Y. (2013). Phylogenetic analysis reveals the evolution and diversification of cyclins in eukaryotes. Mol Phylogenet Evol **66,** 1002-1010.

Marchant, D.B., Chen, G., Cai, S., Chen, F., Schafran, P., Jenkins, J., Shu, S., Plott, C., Webber, J., Lovell, J.T., He, G., Sandor, L., Williams, M., Rajasekar, S., Healey, A., Barry, K., Zhang, Y., Sessa, E., Dhakal, R.R., Wolf, P.G., Harkess, A., Li, F.W., Rossner, C., Becker, A., Gramzow, L., Xue, D., Wu, Y., Tong, T., Wang, Y., Dai, F., Hua, S., Wang, H., Xu, S., Xu, F., Duan, H., Theissen, G., McKain, M.R., Li, Z., McKibben, M.T.W., Barker, M.S., Schmitz, R.J., Stevenson, D.W., Zumajo-Cardona, C., Ambrose, B.A., Leebens-Mack, J.H., Grimwood, J., Schmutz, J., Soltis, P.S., Soltis, D.E., and Chen, Z.H. (2022). Dynamic genome evolution in a model fern. Nat Plants **8,** 1038-1051.

Martinez-Alonso, D., and Malumbres, M. (2020). Mammalian cell cycle cyclins. Semin Cell Dev Biol **107,** 28-35.

Matsuzaki, M., Misumi, O., Shin, I.T., Maruyama, S., Takahara, M., Miyagishima, S.Y., Mori, T., Nishida, K., Yagisawa, F., Nishida, K., Yoshida, Y., Nishimura, Y., Nakao, S., Kobayashi, T., Momoyama, Y., Higashiyama, T., Minoda, A., Sano, M., Nomoto, H., Oishi, K., Hayashi, H., Ohta, F., Nishizaka, S., Haga, S., Miura, S., Morishita, T., Kabeya, Y., Terasawa, K., Suzuki, Y., Ishii, Y., Asakawa, S., Takano, H., Ohta, N., Kuroiwa, H., Tanaka, K., Shimizu, N., Sugano, S., Sato, N., Nozaki, H., Ogasawara, N., Kohara, Y., and Kuroiwa, T. (2004). Genome sequence of the ultrasmall unicellular red alga Cyanidioschyzon merolae 10D. Nature **428,** 653-657.

Menges, M., de Jager, S.M., Gruissem, W., and Murray, J.A. (2005). Global analysis of the core cell cycle regulators of Arabidopsis identifies novel genes, reveals multiple and highly specific profiles of expression and provides a coherent model for plant cell cycle control. Plant J **41,** 546-566.

Menges, M., Samland, A.K., Planchais, S., and Murray, J.A. (2006). The D-type cyclin CYCD3;1 is limiting for the G1-to-S-phase transition in Arabidopsis. Plant Cell **18,** 893-906.

1083 **Merchant, S.S., Prochnik, S.E., Vallon, O., Harris, E.H., Karpowicz, S.J., Witman,**
1084 **G.B., Terry, A., Salamov, A., Fritz-Laylin, L.K., Marechal-Drouard, L., Marshall,**
1085 **W.F., Qu, L.H., Nelson, D.R., Sanderfoot, A.A., Spalding, M.H., Kapitonov,**
1086 **V.V., Ren, Q., Ferris, P., Lindquist, E., Shapiro, H., Lucas, S.M., Grimwood, J.,**
1087 **Schmutz, J., Cardol, P., Cerutti, H., Chanfreau, G., Chen, C.L., Cognat, V.,**
1088 **Croft, M.T., Dent, R., Dutcher, S., Fernandez, E., Fukuzawa, H., Gonzalez-**
1089 **Ballester, D., Gonzalez-Halphen, D., Hallmann, A., Hanikenne, M., Hippler,**
1090 **M., Inwood, W., Jabbari, K., Kalanon, M., Kuras, R., Lefebvre, P.A., Lemaire,**
1091 **S.D., Lobanov, A.V., Lohr, M., Manuell, A., Meier, I., Mets, L., Mittag, M.,**
1092 **Mittelmeier, T., Moroney, J.V., Moseley, J., Napoli, C., Nedelcu, A.M., Niyogi,**
1093 **K., Novoselov, S.V., Paulsen, I.T., Pazour, G., Purton, S., Ral, J.P., Riano-**
1094 **Pachon, D.M., Riekhof, W., Rymarquis, L., Schroda, M., Stern, D., Umen, J.,**
1095 **Willows, R., Wilson, N., Zimmer, S.L., Allmer, J., Balk, J., Bisova, K., Chen, C.J.,**
1096 **Elias, M., Gendler, K., Hauser, C., Lamb, M.R., Ledford, H., Long, J.C.,**
1097 **Minagawa, J., Page, M.D., Pan, J., Pootakham, W., Roje, S., Rose, A.,**
1098 **Stahlberg, E., Terauchi, A.M., Yang, P., Ball, S., Bowler, C., Dieckmann, C.L.,**
1099 **Gladyshev, V.N., Green, P., Jorgensen, R., Mayfield, S., Mueller-Roeber, B.,**
1100 **Rajamani, S., Sayre, R.T., Brokstein, P., Dubchak, I., Goodstein, D., Hornick,**
1101 **L., Huang, Y.W., Jhaveri, J., Luo, Y., Martinez, D., Ngau, W.C., Otillar, B.,**
1102 **Poliakov, A., Porter, A., Szajkowski, L., Werner, G., Zhou, K., Grigoriev, I.V.,**
1103 **Rokhsar, D.S., and Grossman, A.R.** (2007). The Chlamydomonas genome
1104 reveals the evolution of key animal and plant functions. Science **318,** 245-250.
1105 **Minh, B.Q., Schmidt, H.A., Chernomor, O., Schrempf, D., Woodhams, M.D., von**
1106 **Haeseler, A., and Lanfear, R.** (2020). IQ-TREE 2: New Models and Efficient
1107 Methods for Phylogenetic Inference in the Genomic Era. Mol Biol Evol **37,** 1530-
1108 1534.
1109 **Mironov, V.V., De Veylder, L., Van Montagu, M., and Inze, D.** (1999). Cyclin-dependent
1110 kinases and cell division in plants- the nexus. Plant Cell **11,** 509-522.
1111 **Montgomery, S.A., Tanizawa, Y., Galik, B., Wang, N., Ito, T., Mochizuki, T.,**
1112 **Akimcheva, S., Bowman, J.L., Cognat, V., Marechal-Drouard, L., Ekker, H.,**
1113 **Hong, S.F., Kohchi, T., Lin, S.S., Liu, L.D., Nakamura, Y., Valeeva, L.R.,**
1114 **Shakirov, E.V., Shippen, D.E., Wei, W.L., Yagura, M., Yamaoka, S., Yamato,**
1115 **K.T., Liu, C., and Berger, F.** (2020). Chromatin Organization in Early Land Plants
1116 Reveals an Ancestral Association between H3K27me3, Transposons, and
1117 Constitutive Heterochromatin. Curr Biol **30,** 573-588 e577.
1118 **Nagai, I.** (1919). Induced Adventitious Growth in the Gemnnae of Marchanti. The
1119 Botanical Magazine **33,** 99-109.
1120 **Naito, Y., Hino, K., Bono, H., and Ui-Tei, K.** (2015). CRISPRdirect: software for designing
1121 CRISPR/Cas guide RNA with reduced off-target sites. Bioinformatics **31,** 1120-
1122 1123.
1123 **Nishihama, R., Ishida, S., Urawa, H., Kamei, Y., and Kohchi, T.** (2016). Conditional
1124 Gene Expression/Deletion Systems for Marchantia polymorpha Using its Own
1125 Heat-Shock Promoter and Cre/loxP-Mediated Site-Specific Recombination. Plant
1126 Cell Physiol **57,** 271-280.
1127 **Nishihama, R., Ishizaki, K., Hosaka, M., Matsuda, Y., Kubota, A., and Kohchi, T.**
1128 (2015). Phytochrome-mediated regulation of cell division and growth during

regeneration and sporeling development in the liverwort Marchantia polymorpha. J Plant Res **128,** 407-421.

Nishiyama, T., Sakayama, H., de Vries, J., Buschmann, H., Saint-Marcoux, D., Ullrich, K.K., Haas, F.B., Vanderstraeten, L., Becker, D., Lang, D., Vosolsobe, S., Rombauts, S., Wilhelmsson, P.K.I., Janitza, P., Kern, R., Heyl, A., Rumpler, F., Villalobos, L., Clay, J.M., Skokan, R., Toyoda, A., Suzuki, Y., Kagoshima, H., Schijlen, E., Tajeshwar, N., Catarino, B., Hetherington, A.J., Saltykova, A., Bonnot, C., Breuninger, H., Symeonidi, A., Radhakrishnan, G.V., Van Nieuwerburgh, F., Deforce, D., Chang, C., Karol, K.G., Hedrich, R., Ulvskov, P., Glockner, G., Delwiche, C.F., Petrasek, J., Van de Peer, Y., Friml, J., Beilby, M., Dolan, L., Kohara, Y., Sugano, S., Fujiyama, A., Delaux, P.M., Quint, M., Theissen, G., Hagemann, M., Harholt, J., Dunand, C., Zachgo, S., Langdale, J., Maumus, F., Van Der Straeten, D., Gould, S.B., and Rensing, S.A. (2018). The Chara Genome: Secondary Complexity and Implications for Plant Terrestrialization. Cell **174,** 448-464 e424.

Nowack, M.K., Harashima, H., Dissmeyer, N., Zhao, X., Bouyer, D., Weimer, A.K., De Winter, F., Yang, F., and Schnittger, A. (2012). Genetic framework of cyclin-dependent kinase function in Arabidopsis. Dev Cell **22,** 1030-1040.

Palenik, B., Grimwood, J., Aerts, A., Rouze, P., Salamov, A., Putnam, N., Dupont, C., Jorgensen, R., Derelle, E., Rombauts, S., Zhou, K., Otillar, R., Merchant, S.S., Podell, S., Gaasterland, T., Napoli, C., Gendler, K., Manuell, A., Tai, V., Vallon, O., Piganeau, G., Jancek, S., Heijde, M., Jabbari, K., Bowler, C., Lohr, M., Robbens, S., Werner, G., Dubchak, I., Pazour, G.J., Ren, Q., Paulsen, I., Delwiche, C., Schmutz, J., Rokhsar, D., Van de Peer, Y., Moreau, H., and Grigoriev, I.V. (2007). The tiny eukaryote Ostreococcus provides genomic insights into the paradox of plankton speciation. Proc Natl Acad Sci U S A **104,** 7705-7710.

Patron, N.J., Orzaez, D., Marillonnet, S., Warzecha, H., Matthewman, C., Youles, M., Raitskin, O., Leveau, A., Farre, G., Rogers, C., Smith, A., Hibberd, J., Webb, A.A., Locke, J., Schornack, S., Ajioka, J., Baulcombe, D.C., Zipfel, C., Kamoun, S., Jones, J.D., Kuhn, H., Robatzek, S., Van Esse, H.P., Sanders, D., Oldroyd, G., Martin, C., Field, R., O'Connor, S., Fox, S., Wulff, B., Miller, B., Breakspear, A., Radhakrishnan, G., Delaux, P.M., Loque, D., Granell, A., Tissier, A., Shih, P., Brutnell, T.P., Quick, W.P., Rischer, H., Fraser, P.D., Aharoni, A., Raines, C., South, P.F., Ane, J.M., Hamberger, B.R., Langdale, J., Stougaard, J., Bouwmeester, H., Udvardi, M., Murray, J.A., Ntoukakis, V., Schafer, P., Denby, K., Edwards, K.J., Osbourn, A., and Haseloff, J. (2015). Standards for plant synthetic biology: a common syntax for exchange of DNA parts. New Phytol **208,** 13-19.

Pecani, K., Lieberman, K., Tajima-Shirasaki, N., Onishi, M., and Cross, F.R. (2022). Control of division in Chlamydomonas by cyclin B/CDKB1 and the anaphase-promoting complex. PLoS Genet **18,** e1009997.

Peramuna, A., Lopez, C.Q., Rios, F.J.A., Bae, H., Fangel, J.U., Batth, R., Harholt, J., and Simonsen, H.T. (2023). Overexpression of Physcomitrium patens cell cycle regulators leads to larger gametophytes. Sci Rep **13,** 4301.

Procter, J.B., Carstairs, G.M., Soares, B., Mourao, K., Ofoegbu, T.C., Barton, D., Lui, L., Menard, A., Sherstnev, N., Roldan-Martinez, D., Duce, S., Martin, D.M.A.,

1176 **and Barton, G.J.** (2021). Alignment of Biological Sequences with Jalview. Methods
1177 Mol Biol **2231,** 203-224.
1178 **Quevillon, E., Silventoinen, V., Pillai, S., Harte, N., Mulder, N., Apweiler, R., and**
1179 **Lopez, R.** (2005). InterProScan: protein domains identifier. Nucleic Acids Res **33,**
1180 W116-120.
1181 **Radhakrishnan, G.V., Keller, J., Rich, M.K., Vernie, T., Mbadinga Mbadinga, D.L.,**
1182 **Vigneron, N., Cottret, L., Clemente, H.S., Libourel, C., Cheema, J., Linde,**
1183 **A.M., Eklund, D.M., Cheng, S., Wong, G.K.S., Lagercrantz, U., Li, F.W.,**
1184 **Oldroyd, G.E.D., and Delaux, P.M.** (2020). An ancestral signalling pathway is
1185 conserved in intracellular symbioses-forming plant lineages. Nat Plants **6,** 280-
1186 289.
1187 **Rauber, R., Cabreira, C., de Freitas, L.B., Turchetto-Zolet, A.C., and Margis-Pinheiro,**
1188 **M.** (2016). The evolutionary history of the E2F and DEL genes in Viridiplantae. Mol
1189 Phylogenet Evol **99,** 225-234.
1190 **Romani, F., Sauret-Gueto, S., Rebmann, M., Annese, D., Bonter, I., Tomaselli, M.,**
1191 **Dierschke, T., Delmans, M., Frangedakis, E., Silvestri, L., Rever, J., Bowman,**
1192 **J.L., Romani, I., and Haseloff, J.** (2024). The landscape of transcription factor
1193 promoter activity during vegetative development in Marchantia. Plant Cell **36,**
1194 2140-2159.
1195 **Sakamoto, Y., Ishimoto, A., Sakai, Y., Sato, M., Nishihama, R., Abe, K., Sano, Y.,**
1196 **Furuichi, T., Tsuji, H., Kohchi, T., and Matsunaga, S.** (2022). Improved clearing
1197 method contributes to deep imaging of plant organs. Commun Biol **5,** 12.
1198 **Sauret-Gueto, S., Frangedakis, E., Silvestri, L., Rebmann, M., Tomaselli, M., Markel,**
1199 **K., Delmans, M., West, A., Patron, N.J., and Haseloff, J.** (2020). Systematic
1200 Tools for Reprogramming Plant Gene Expression in a Simple Model, Marchantia
1201 polymorpha. ACS Synth Biol **9,** 864-882.
1202 **Schnittger, A., and De Veylder, L.** (2018). The Dual Face of Cyclin B1. Trends Plant Sci
1203 **23,** 475-478.
1204 **Schnittger, A., Schobinger, U., Stierhof, Y.D., and Hulskamp, M.** (2002a). Ectopic B-
1205 type cyclin expression induces mitotic cycles in endoreduplicating Arabidopsis
1206 trichomes. Curr Biol **12,** 415-420.
1207 **Schnittger, A., Schobinger, U., Bouyer, D., Weinl, C., Stierhof, Y.D., and Hulskamp,**
1208 **M.** (2002b). Ectopic D-type cyclin expression induces not only DNA replication but
1209 also cell division in Arabidopsis trichomes. Proc Natl Acad Sci U S A **99,** 6410-
1210 6415.
1211 **Schween, G., Gorr, G., Hohe, A., and Reski, R.** (2008). Unique Tissue-Specific Cell
1212 Cycle in Physcomitrella. Plant Biology **5,** 50-58.
1213 **Siligato, R., Wang, X., Yadav, S.R., Lehesranta, S., Ma, G., Ursache, R., Sevilem, I.,**
1214 **Zhang, J., Gorte, M., Prasad, K., Wrzaczek, M., Heidstra, R., Murphy, A.,**
1215 **Scheres, B., and Mahonen, A.P.** (2016). MultiSite Gateway-Compatible Cell
1216 Type-Specific Gene-Inducible System for Plants. Plant Physiol **170,** 627-641.
1217 **Sozzani, R., Maggio, C., Varotto, S., Canova, S., Bergounioux, C., Albani, D., and**
1218 **Cella, R.** (2006). Interplay between Arabidopsis activating factors E2Fb and E2Fa
1219 in cell cycle progression and development. Plant Physiol **140,** 1355-1366.
1220 **Sugano, S.S., Nishihama, R., Shirakawa, M., Takagi, J., Matsuda, Y., Ishida, S.,**
1221 **Shimada, T., Hara-Nishimura, I., Osakabe, K., and Kohchi, T.** (2018). Efficient

CRISPR/Cas9-based genome editing and its application to conditional genetic analysis in Marchantia polymorpha. PLoS One **13,** e0205117.

Takahashi, I., Kojima, S., Sakaguchi, N., Umeda-Hara, C., and Umeda, M. (2010). Two Arabidopsis cyclin A3s possess G1 cyclin-like features. Plant Cell Rep **29,** 307-315.

Toyoshima, F., Moriguchi, T., Wada, A., Fukuda, M., and Nishida, E. (1998). Nuclear export of cyclin B1 and its possible role in the DNA damage-induced G2 checkpoint. EMBO J **17,** 2728-2735.

Tse, S.W., Annese, D., Romani, F., Guzman-Chavez, F., Bonter, I., Forestier, E., Frangedakis, E., and Haseloff, J. (2024). Optimising promoters and subcellular localisation for constitutive transgene expression in Marchantia polymorpha. Plant Cell Physiol.

Tulin, F., and Cross, F.R. (2014). A microbial avenue to cell cycle control in the plant superkingdom. Plant Cell **26,** 4019-4038.

Tulin, F., and Cross, F.R. (2015). Cyclin-Dependent Kinase Regulation of Diurnal Transcription in Chlamydomonas. Plant Cell **27,** 2727-2742.

Wang, L., Wan, M.C., Liao, R.Y., Xu, J., Xu, Z.G., Xue, H.C., Mai, Y.X., and Wang, J.W. (2023). The maturation and aging trajectory of Marchantia polymorpha at single-cell resolution. Dev Cell.

Wang, W., Haberer, G., Gundlach, H., Glasser, C., Nussbaumer, T., Luo, M.C., Lomsadze, A., Borodovsky, M., Kerstetter, R.A., Shanklin, J., Byrant, D.W., Mockler, T.C., Appenroth, K.J., Grimwood, J., Jenkins, J., Chow, J., Choi, C., Adam, C., Cao, X.H., Fuchs, J., Schubert, I., Rokhsar, D., Schmutz, J., Michael, T.P., Mayer, K.F., and Messing, J. (2014). The Spirodela polyrhiza genome reveals insights into its neotenous reduction fast growth and aquatic lifestyle. Nat Commun **5,** 3311.

Willems, A., Heyman, J., Eekhout, T., Achon, I., Pedroza-Garcia, J.A., Zhu, T., Li, L., Vercauteren, I., Van den Daele, H., van de Cotte, B., De Smet, I., and De Veylder, L. (2020). The Cyclin CYCA3;4 Is a Postprophase Target of the APC/C(CCS52A2) E3-Ligase Controlling Formative Cell Divisions in Arabidopsis. Plant Cell **32,** 2979-2996.

Zhang, T.Q., Chen, Y., and Wang, J.W. (2021). A single-cell analysis of the Arabidopsis vegetative shoot apex. Dev Cell **56,** 1056-1074 e1058.